

Quantum Theory of Magnetism: Itinerant-Electron Systems and the Kondo Effect

When we think about magnetism in an itinerant electron system, a Sommerfeld model immediately comes to mind. However, we also immediately realize that, depending on the sign of the susceptibility χ , a noninteracting electron gas can exhibit paramagnetism or diamagnetism, but it can never develop a spontaneous magnetic moment: $\mathbf{M}|_{\mathbf{B}=0} = 0$.

What then gives rise to magnetism in itinerant electron systems? Again, it must be that Coulomb repulsion between electrons is responsible for magnetism whenever it arises in itinerant-electron systems. At the outset, this might seem odd, since the Coulomb interaction is spin independent. How then can it lead to a spontaneous magnetic moment? To arrive at a reasonable explanation, we shall introduce the Stoner model.

24.1 Stoner Mean-Field Theory: Ferromagnetic Case

Stoner developed a very simple picture of ferromagnetism based on the competition between the kinetic energy cost of making the \uparrow and \downarrow spin electron numbers different and the corresponding gain in exchange energy. The basic idea can be explained as follows.

In the absence of Coulomb interaction, the Pauli principle allows double occupancy of each energy level with electrons of opposite spins, up to the Fermi energy. If, instead, we make the number of \uparrow and \downarrow electrons unequal, we will have to occupy levels above the designated Fermi energy. However, in the presence of Coulomb interaction, such an unequal configuration results in a decrease of exchange energy. In the extreme case of complete polarization, shown in Figure 24.1, the exchange energy cost becomes zero. To make the argument more precise, we consider a system with equal \uparrow and \downarrow filling up to the same E_F . The density of \uparrow or \downarrow electrons is equal to n . We compute the change in energy that results from a reduction in the density of \downarrow spin electrons by δn and at the same time an increase the number of \uparrow spin electrons by δn . The potential energy changes by

$$\Delta V = U (n + \delta n) (n - \delta n) - U n^2 = -U (\delta n)^2.$$

Placing an extra δn electrons into the \uparrow group requires occupying energy levels above E_F . With the density of states $\mathcal{D}(E) = dN/dE$, we have $\delta n = \mathcal{D}(E) \delta E$. This delineates the range of energies above E_F filled by δn . It also gives the energy range of emptied levels

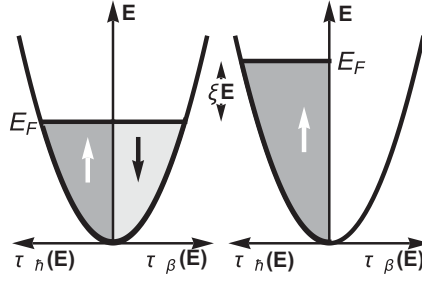


Figure 24.1 Increase in kinetic energy.

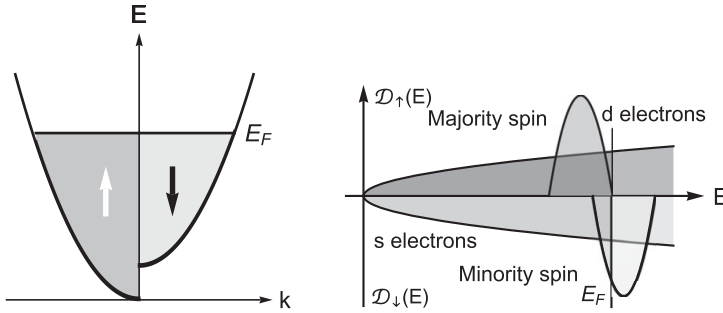


Figure 24.2 Left: Stoner criterion. Right: a more typical rendering of an itinerant ferromagnet is given on the right, showing the high density of states (DOS) of a 3d system.

below E_F that used to be occupied by down-spin electrons. The net result of this process is to shift δn electrons up in energy by an amount δE . The change in the kinetic energy is then

$$\delta T = \delta n \delta E = \frac{1}{\mathcal{D}(E)} (\delta n)^2.$$

Combining these two contributions,

$$\delta E = \delta T + \delta V = \left(\frac{1}{\mathcal{D}(E)} - U \right) (\delta n)^2 = (1 - U \mathcal{D}(E)) \frac{(\delta n)^2}{\mathcal{D}(E)}.$$

It is clear that for $U \mathcal{D}(E) > 1$ the total energy change $\delta E < 0$, so it is favorable to have different \uparrow and \downarrow electron densities, which favors ferromagnetism. This is called the Stoner criterion (see Figure 24.2). It tells us that magnetism is favored by large electron interactions. As we shall see, this simple calculation yields results in precise agreement with mean-field theory.

24.1.1 Mean-Field Hubbard Model

The simplest model that can describe itinerant magnetism is the Hubbard model:

$$\mathcal{H} = -t \sum_{\langle ij \rangle, \sigma} \left(c_{i\sigma}^\dagger c_{j\sigma} + c_{j\sigma}^\dagger c_{i\sigma} \right) + U \sum_i n_{i\uparrow} n_{i\downarrow} - \mu_B B \sum_i (n_{i\uparrow} - n_{i\downarrow}).$$

As is quite clear by now, we cannot devise general methods to solve for the exact ground state of such an interacting many-body Hamiltonian. However, we can solve this problem, approximately, using a mean-field theory due to Stoner. As we have stated, the Hubbard model accounts for onsite Coulomb interactions only, and hence it has a constant value in reciprocal space. Thus, we write the Hubbard Hamiltonian in k -space as

$$\mathcal{H} = \sum_{\mathbf{k}\sigma} \varepsilon_{\mathbf{k}} c_{\mathbf{k}\sigma}^\dagger c_{\mathbf{k}\sigma} + \frac{U}{2\Omega} \sum_{\substack{\mathbf{k}\mathbf{k}'\mathbf{q} \\ \sigma\sigma'}} c_{\mathbf{k}+\mathbf{q},\sigma}^\dagger c_{\mathbf{k}'-\mathbf{q},\sigma'}^\dagger c_{\mathbf{k}'\sigma'} c_{\mathbf{k}\sigma}. \quad (24.1)$$

We apply the Hartree–Fock approximation to this model, but search for a ferromagnetic solution by allowing for the expectation values to depend on the direction of the spin. We substitute

$$\begin{aligned} c_{\mathbf{k}+\mathbf{q},\sigma}^\dagger c_{\mathbf{k}'-\mathbf{q},\sigma'}^\dagger c_{\mathbf{k}'\sigma'} c_{\mathbf{k}\sigma} &= 2 \left\langle c_{\mathbf{k}+\mathbf{q},\sigma}^\dagger c_{\mathbf{k}\sigma} \right\rangle c_{\mathbf{k}'-\mathbf{q},\sigma'}^\dagger c_{\mathbf{k}'\sigma'} - 2 \left\langle c_{\mathbf{k}+\mathbf{q},\sigma}^\dagger c_{\mathbf{k}'\sigma'} \right\rangle c_{\mathbf{k}'-\mathbf{q},\sigma'}^\dagger c_{\mathbf{k}\sigma} \\ &\quad - \left\langle c_{\mathbf{k}+\mathbf{q},\sigma}^\dagger c_{\mathbf{k}\sigma} \right\rangle \left\langle c_{\mathbf{k}'-\mathbf{q},\sigma'}^\dagger c_{\mathbf{k}'\sigma'} \right\rangle + \left\langle c_{\mathbf{k}+\mathbf{q},\sigma}^\dagger c_{\mathbf{k}'\sigma'} \right\rangle \left\langle c_{\mathbf{k}'-\mathbf{q},\sigma'}^\dagger c_{\mathbf{k}\sigma} \right\rangle \end{aligned}$$

in the interaction component of (24.1), and we obtain the mean-field interaction Hamiltonian

$$\begin{aligned} V_{\text{int}}^{\text{MF}} &= \frac{U}{\Omega} \sum_{\substack{\mathbf{k}\mathbf{k}'\mathbf{q} \\ \sigma\sigma'}} c_{\mathbf{k}+\mathbf{q},\sigma}^\dagger \left\langle c_{\mathbf{k}'-\mathbf{q},\sigma'}^\dagger c_{\mathbf{k}'\sigma'} \right\rangle c_{\mathbf{k}\sigma} - \frac{U}{\Omega} \sum_{\substack{\mathbf{k}\mathbf{k}'\mathbf{q} \\ \sigma\sigma'}} \left\langle c_{\mathbf{k}+\mathbf{q},\sigma}^\dagger c_{\mathbf{k}'\sigma'} \right\rangle c_{\mathbf{k}'-\mathbf{q},\sigma'}^\dagger c_{\mathbf{k}\sigma} \\ &\quad - \frac{U}{2\Omega} \sum_{\substack{\mathbf{k}\mathbf{k}'\mathbf{q} \\ \sigma\sigma'}} \left[\left\langle c_{\mathbf{k}+\mathbf{q},\sigma}^\dagger c_{\mathbf{k}\sigma} \right\rangle \left\langle c_{\mathbf{k}'-\mathbf{q},\sigma'}^\dagger c_{\mathbf{k}'\sigma'} \right\rangle - \left\langle c_{\mathbf{k}+\mathbf{q},\sigma}^\dagger c_{\mathbf{k}'\sigma'} \right\rangle \left\langle c_{\mathbf{k}'-\mathbf{q},\sigma'}^\dagger c_{\mathbf{k}\sigma} \right\rangle \right]. \end{aligned}$$

With the mean-field parameters defined as

$$\left\langle c_{\mathbf{k}\uparrow}^\dagger c_{\mathbf{k}'\uparrow} \right\rangle = \delta_{\mathbf{k}\mathbf{k}'} n_{\mathbf{k}\uparrow}, \quad \left\langle c_{\mathbf{k}\downarrow}^\dagger c_{\mathbf{k}'\downarrow} \right\rangle = \delta_{\mathbf{k}\mathbf{k}'} n_{\mathbf{k}\downarrow} \quad (24.2)$$

and the spin densities

$$\bar{n}_\sigma = \frac{1}{\Omega} \sum_{\mathbf{k}} \left\langle c_{\mathbf{k}\sigma}^\dagger c_{\mathbf{k}\sigma} \right\rangle,$$

we get

$$V_{\text{int}}^{\text{MF}} = U \sum_{\mathbf{k}\sigma\sigma'} c_{\mathbf{k}\sigma}^\dagger c_{\mathbf{k}\sigma} [\bar{n}_{\sigma'} - \bar{n}_\sigma \delta_{\sigma\sigma'}] - U\Omega \sum_{\sigma\sigma'} \bar{n}_{\sigma'} \bar{n}_\sigma + U\Omega \sum_{\sigma} \bar{n}_\sigma^2.$$

The full Stoner mean-field Hamiltonian is now given by

$$\begin{aligned}\mathcal{H}_{\text{MF}} &= \sum_{\mathbf{k}\sigma} \mathcal{E}_{\mathbf{k}\sigma}^{\text{MF}} c_{\mathbf{k}\sigma}^\dagger c_{\mathbf{k}\sigma} - U\Omega \sum_{\sigma\sigma'} \bar{n}_{\sigma'} \bar{n}_{\sigma} + U\Omega \sum_{\sigma} \bar{n}_{\sigma}^2 \\ \mathcal{E}_{\mathbf{k}\sigma}^{\text{MF}} &= \varepsilon_{\mathbf{k}} + U (\bar{n}_{\uparrow} + \bar{n}_{\downarrow} - \bar{n}_{\sigma}) = \varepsilon_{\mathbf{k}} + U \bar{n}_{\bar{\sigma}}.\end{aligned}\quad (24.3)$$

We obtain the $T = 0$ mean-field solution via the self-consistency equations

$$\bar{n}_{\sigma} = \frac{1}{\Omega} \sum_{\mathbf{k}} \langle c_{\mathbf{k}\sigma}^\dagger c_{\mathbf{k}\sigma} \rangle = \int \frac{d\mathbf{k}}{(2\pi)^3} \Theta \left(\mu - \frac{\hbar^2 k^2}{2m} - U \bar{n}_{\bar{\sigma}} \right) = \frac{1}{6\pi^2} k_{F\sigma}^3,$$

where $\frac{\hbar^2 k_{F\sigma}^2}{2m} + U \bar{n}_{\bar{\sigma}} = \mu$, leading to

$$\frac{\hbar^2}{2m} (6\pi^2)^{2/3} \bar{n}_{\uparrow}^{2/3} + U \bar{n}_{\downarrow} = \frac{\hbar^2}{2m} (6\pi^2)^{2/3} \bar{n}_{\downarrow}^{2/3} + U \bar{n}_{\uparrow} = \mu. \quad (24.4)$$

Defining the quantities

$$\bar{n} = \bar{n}_{\uparrow} + \bar{n}_{\downarrow}, \quad \zeta = \frac{\bar{n}_{\uparrow} - \bar{n}_{\downarrow}}{\bar{n}}, \quad \gamma = \frac{2mU \bar{n}^{1/3}}{(6\pi^2)^{2/3} \hbar^2}$$

and rearranging the self-consistency conditions (24.4), we get

$$\bar{n}_{\uparrow}^{2/3} - \bar{n}_{\downarrow}^{2/3} = \frac{2mU}{(6\pi^2)^{2/3} \hbar^2} (\bar{n}_{\uparrow} - \bar{n}_{\downarrow}) \Rightarrow (1 + \zeta)^{2/3} - (1 - \zeta)^{2/3} = \gamma \zeta. \quad (24.5)$$

A graphic solution of (24.5) is depicted in Figure 24.3. It shows three solution regimes:

$$\begin{aligned}\gamma < \frac{4}{3} : & \quad \text{Isotropic solution (normal state)} & \quad \zeta = 0 \\ \frac{4}{3} < \gamma < 2^{2/3} : & \quad \text{Partial polarization (weak ferromagnet)} & \quad 0 < \zeta < 1 \\ \gamma > 2^{2/3} : & \quad \text{Full polarization (strong ferromagnet)} & \quad \zeta = 1\end{aligned}$$

We note that the initial slope of the lhs is $4/3$, and its value at $\zeta = 1$ is $2^{2/3}$, which signals complete polarization. The different solutions are sketched in Figure 24.4.

24.1.2 Temperature Dependence of Magnetization in Mean Field

We write the site occupancy $n_{i\sigma}$ as

$$n_{i\sigma} = \langle n_{\sigma} \rangle + \delta n_{i\sigma}, \quad (24.6)$$

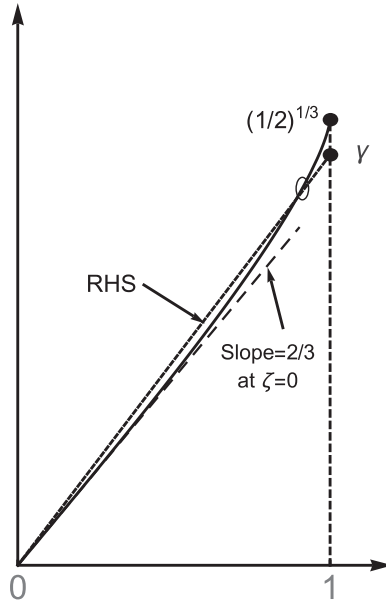


Figure 24.3 Plot of the two sides of (24.5).

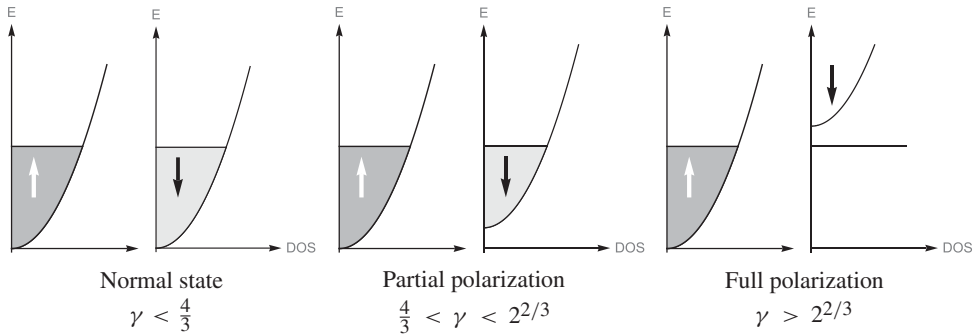


Figure 24.4 The three possible solutions of the Stoner model. The polarization is thus a function of the interaction strength; the stronger the interaction, the larger the polarization. The Stoner model provides a clear physical picture for how the exchange interactions induce a ferromagnetic phase transition in a metal with strong onsite interactions.

where $\langle n_{i\sigma} \rangle$ is the thermodynamic average, and $\delta n_{i\sigma}$ the fluctuating component, such that $|\delta n_{i\sigma}|^2 \ll \langle n_{i\sigma} \rangle^2$. Substituting in the Hubbard Hamiltonian, we get

$$\begin{aligned}
 \mathcal{H}^{\text{MF}} &= \sum_{\mathbf{k}\sigma} \varepsilon_{\mathbf{k}} c_{\mathbf{k}\sigma}^\dagger c_{\mathbf{k}\sigma} + U \sum_i \left[n_{i\uparrow} \langle n_{i\downarrow} \rangle + n_{i\downarrow} \langle n_{i\uparrow} \rangle + \langle n_{i\uparrow} \rangle \langle n_{i\downarrow} \rangle \right] \\
 &= \sum_{\mathbf{k}\sigma} \left(\varepsilon_{\mathbf{k}} + U \langle n_{\bar{\sigma}} \rangle \right) c_{\mathbf{k}\sigma}^\dagger c_{\mathbf{k}\sigma} + U N \langle n_{\uparrow} \rangle \langle n_{\downarrow} \rangle,
 \end{aligned} \tag{24.7}$$

The advantage of this approximation is that the many-body problem is now reduced to an effective one-particle problem, where only the mean electron interaction is taken into account. We express $\langle n_\sigma \rangle$ as

$$\begin{aligned}\langle n_\sigma \rangle &= \frac{1}{N} \sum_{\mathbf{k}} \langle c_{\mathbf{k}\sigma}^\dagger c_{\mathbf{k}\sigma} \rangle = \int d\varepsilon \frac{1}{N} \sum_{\mathbf{k}} \delta(\varepsilon - \varepsilon_{\mathbf{k}} - U \langle n_{\bar{\sigma}} \rangle) n_F(\varepsilon) \\ &= \int d\varepsilon \frac{1}{2} \mathcal{D}(\varepsilon - U \langle n_{\bar{\sigma}} \rangle) n_F(\varepsilon).\end{aligned}\quad (24.8)$$

To solve for the $\langle n_\sigma \rangle$ s self-consistently, we introduce the average occupancy, \bar{n} , and average spin polarization, m

$$\left. \begin{aligned}\bar{n} &= \langle n_\downarrow \rangle + \langle n_\uparrow \rangle \\ m &= \langle n_\uparrow \rangle - \langle n_\downarrow \rangle\end{aligned} \right\} \Rightarrow \langle n_\sigma \rangle = \frac{1}{2} (\bar{n} + \sigma m) \quad (24.9)$$

and obtain

$$\begin{aligned}\bar{n} &= \frac{1}{2} \int d\varepsilon \left[\mathcal{D}(\varepsilon - U \langle n_\downarrow \rangle) + \mathcal{D}(\varepsilon - U \langle n_\uparrow \rangle) \right] n_F(\varepsilon) \\ &= \frac{1}{2} \sum_{\sigma} \int d\varepsilon \mathcal{D} \left(\varepsilon - \frac{U \bar{n}}{2} - \sigma \frac{Um}{2} \right) n_F(\varepsilon)\end{aligned}\quad (24.10)$$

$$\begin{aligned}m &= \frac{1}{2} \int d\varepsilon \left[\mathcal{D}(\varepsilon - U \langle n_\downarrow \rangle) - \mathcal{D}(\varepsilon - U \langle n_\uparrow \rangle) \right] n_F(\varepsilon) \\ &= -\frac{1}{2} \sum_{\sigma} \sigma \int d\varepsilon \mathcal{D} \left(\varepsilon - \frac{U \bar{n}}{2} - \sigma \frac{Um}{2} \right) n_F(\varepsilon),\end{aligned}\quad (24.11)$$

which presents two coupled equations that can be solved approximately for $m \ll \bar{n}$, by allowing a change in the chemical potential μ that depends on temperature and polarization:

$$\mu(m, T) = \varepsilon_F + \frac{U \bar{n}}{2} + \Delta\mu(m, T) = \bar{\varepsilon}_F + \Delta\mu(m, T).$$

For small m , T , and

$$n_F(\varepsilon, T) = \frac{1}{e^{\beta(\varepsilon - \mu(m, T))} + 1} = n_F(\varepsilon, 0) + \left. \frac{\partial n_F}{\partial \mu} \right|_{\mu = \bar{\varepsilon}_F} \Delta\mu(m, T) + \frac{\partial n_F}{\partial T} k_B T, \quad k_B T \ll \varepsilon_F,$$

we expand (24.10) as

$$\begin{aligned}\bar{n} &\simeq \int d\varepsilon \left[\mathcal{D}(\varepsilon) + \frac{1}{2} \left(\frac{Um}{2} \right)^2 \frac{d^2 \mathcal{D}(\varepsilon)}{d\varepsilon^2} + \dots \right] n_F(\varepsilon) \\ &\approx \int_0^{\bar{\varepsilon}_F} d\varepsilon \mathcal{D}(\varepsilon) + \mathcal{D}(\bar{\varepsilon}_F) \Delta\mu + \left[\frac{\pi^2}{6} (k_B T)^2 \frac{d\mathcal{D}(\varepsilon)}{d\varepsilon} + \frac{1}{2} \left(\frac{Um}{2} \right)^2 \frac{d^2 \mathcal{D}(\varepsilon)}{d\varepsilon^2} \right]_{\bar{\varepsilon}_F},\end{aligned}$$

where we used

$$\int_{-\infty}^{\infty} dx x^2 \frac{e^x}{(e^x + 1)^2} = \frac{\pi^2}{3}$$

and we expanded $\mathcal{D}(\varepsilon)$ around $\bar{\varepsilon}_F$. We note that

$$\int_0^{\bar{\varepsilon}_F} d\varepsilon \mathcal{D}(\varepsilon) = \bar{n}$$

and we obtain

$$\Delta\mu(m, T) = -\frac{\mathcal{D}'(\bar{\varepsilon}_F)}{\mathcal{D}(\bar{\varepsilon}_F)} \left[\frac{\pi^2}{6} (k_B T)^2 + \frac{1}{2} \left(\frac{Um}{2} \right)^2 \right].$$

Next we carry out a similar expansion for m and substitute for $\Delta\mu(m, T)$

$$\begin{aligned} m &\simeq \int d\varepsilon \left[\frac{d\mathcal{D}(\varepsilon)}{d\varepsilon} \frac{Um}{2} + \frac{1}{3!} \left(\frac{Um}{2} \right)^3 \frac{d^3\mathcal{D}(\varepsilon)}{d\varepsilon^3} + \dots \right] n_F(\varepsilon) \\ &\simeq \left[\mathcal{D}(\bar{\varepsilon}_F) + \mathcal{D}'(\bar{\varepsilon}_F) \Delta\mu + \frac{\pi^2}{6} (k_B T)^2 \mathcal{D}''(\bar{\varepsilon}_F) + \frac{1}{3!} \left(\frac{Um}{2} \right)^2 \mathcal{D}''(\bar{\varepsilon}_F) \right] \frac{Um}{2} \\ &= A(\bar{\varepsilon}_F, T) m - B(\bar{\varepsilon}_F) m^3, \end{aligned}$$

where

$$\begin{aligned} A(\bar{\varepsilon}_F, T) &= \frac{\mathcal{D}(\bar{\varepsilon}_F)U}{2} \left\{ 1 - \left[\left(\frac{\mathcal{D}'(\bar{\varepsilon}_F)}{\mathcal{D}(\bar{\varepsilon}_F)} \right)^2 - \frac{\mathcal{D}''(\bar{\varepsilon}_F)}{\mathcal{D}(\bar{\varepsilon}_F)} \right] \frac{\pi^2}{6} (k_B T)^2 \right\} = \frac{\mathcal{D}(\bar{\varepsilon}_F)U}{2} (1 - \alpha T^2) \\ B(\bar{\varepsilon}_F) &= \mathcal{D}(\bar{\varepsilon}_F) \left(\frac{U}{2} \right)^3 \left[\frac{1}{2} \left(\frac{\mathcal{D}'(\bar{\varepsilon}_F)}{\mathcal{D}(\bar{\varepsilon}_F)} \right)^2 - \frac{\mathcal{D}''(\bar{\varepsilon}_F)}{3! \mathcal{D}(\bar{\varepsilon}_F)} \right]. \end{aligned}$$

We find that

$$m^2 = \frac{A-1}{B}, \quad A, B > 0.$$

Thus a nonzero real root exists for $A > 1$, which yields two conditions for a Fermi liquid instability and the emergence of magnetism

$$\begin{cases} U > \frac{2}{\mathcal{D}(\bar{\varepsilon}_F)} = U_c \\ T \leq \frac{1}{\alpha} \sqrt{1 - \frac{U_c}{U}} = T_c, \end{cases}$$

where T_c is the Curie temperature. The emerging magnetization M exhibits a temperature dependence

$$M \propto \sqrt{T_c - T}.$$

24.2 RPA Susceptibility: Stoner Excitations and Spin Waves

We now turn to explore the nature of excitations above the Stoner ground state. Such excitations are described by the dynamical magnetic response contained in the magnetic susceptibility, which we now consider.

24.2.1 The RPA Magnetic Susceptibility

The magnetic susceptibility, $\chi(\mathbf{x}t; \mathbf{x}', t')$, gives the change in spin density in response to an external applied magnetic field:

$$\delta s_\alpha(\mathbf{x}, t) = \sum_\beta \int d\mathbf{x}' \int dt' \chi_{\alpha\beta}(\mathbf{x}t; \mathbf{x}', t') B_\beta(\mathbf{x}', t').$$

The spin density $\mathbf{s}(\mathbf{x})$ is defined as

$$s_\alpha(\mathbf{x}) = \sum_{\sigma, \sigma'} \Psi_\sigma^\dagger(\mathbf{x}) (\sigma^\alpha)_{\sigma\sigma'} \Psi_{\sigma'}(\mathbf{x}),$$

where σ^α are the Pauli matrices. The magnetic field \mathbf{B} enters into the Hamiltonian through the Zeeman coupling,

$$\mathcal{H}_I = -\frac{\hbar}{2} \mu_B g \int d\mathbf{x} B(\mathbf{x}, t) \cdot \mathbf{s}(\mathbf{x}).$$

We can express the spin susceptibility in terms of the retarded spin–spin correlation, or Green function as

$$\chi_{\alpha\beta}(\mathbf{x}, t; \mathbf{x}', t') = i \frac{\mu_B g}{2} \Theta(t - t') \langle [s_\alpha(\mathbf{x}, t), s_\beta(\mathbf{x}', t')] \rangle,$$

where the minus sign characteristic of the Green function is removed by that appearing in \mathcal{H}_I . Transformation to frequency space yields

$$\begin{aligned} \delta s_\alpha(\mathbf{x}, \omega) &= \sum_\beta \int d\mathbf{x}' \chi_{\alpha\beta}(\mathbf{x}, \mathbf{x}', \omega) B_\beta(\mathbf{x}', \omega) \\ \chi_{\alpha\beta}(\mathbf{x}, \mathbf{x}', \omega) &= i \frac{\mu_B g}{2} \int dt e^{i\omega t} \langle [s_\alpha(\mathbf{x}, t), s_\beta(\mathbf{x}', 0)] \rangle. \end{aligned}$$

Moreover, for spatially homogeneous systems, we may carry out a spatial Fourier transform, to obtain

$$\chi_{\alpha\beta}(\mathbf{q}, \omega) = \frac{1}{\Omega} \int d\mathbf{x} d\mathbf{x}' e^{i\mathbf{q} \cdot (\mathbf{x} - \mathbf{x}')} \chi_{\alpha\beta}(\mathbf{x} - \mathbf{x}', \omega).$$

In the plane wave representation, we write

$$\mathbf{s}(\mathbf{x}, t) = \sum_{\mathbf{q}} e^{i\mathbf{q} \cdot \mathbf{x}} \mathbf{s}(\mathbf{q}, t), \quad \Rightarrow \quad s_\alpha(\mathbf{q}, t) = \sum_{\mathbf{k}} c_{\mathbf{k}+\mathbf{q}, s}^\dagger(t) \sigma_{ss'}^\alpha c_{\mathbf{k}, s'}(t),$$

$$s^+(\mathbf{q}, t) = \sum_{\mathbf{k}} c_{\mathbf{k}+\mathbf{q}, \uparrow}^\dagger(t) c_{\mathbf{k}\downarrow}(t), \quad s^-(\mathbf{q}, t) = \sum_{\mathbf{k}} c_{\mathbf{k}+\mathbf{q}, \downarrow}^\dagger(t) c_{\mathbf{k}\uparrow}(t),$$

$$s^z(\mathbf{q}, t) = \frac{1}{2} \sum_{\mathbf{k}} \left(c_{\mathbf{k}+\mathbf{q}, \uparrow}^\dagger(t) c_{\mathbf{k}\uparrow}(t) - c_{\mathbf{k}+\mathbf{q}, \downarrow}^\dagger(t) c_{\mathbf{k}\downarrow}(t) \right).$$

We identify two types of spin susceptibility functions:

- The *transverse* spin susceptibility function, χ^{-+} , which represents the response to a field that couples to the spin-flip (deviation) component of the spin
- The *longitudinal* susceptibility χ^{zz} containing the response to a field that couples to the S_z component

It is particularly interesting to examine the transverse spin fluctuations, or deviations. A uniform transverse spin fluctuation corresponds to a rotation of the magnetization, which costs no energy due to the rotational invariance of the system. If we carry out a slow twist of the magnetization, this costs an energy that goes to zero as the pitch of the twist goes to infinity. The corresponding normal mode is the “Goldstone mode” of the magnet.

For the case we are interested in, namely, ferromagnetic excitations, we shall consider the retarded transverse susceptibility

$$\chi^{-+}(\mathbf{x}, t; 0, 0) = i\Theta(t) \langle [s^{-}(\mathbf{x}, t), s^{+}(0, 0)] \rangle = \sum_{\mathbf{q}} \chi^{-+}(\mathbf{q}, t).$$

We find that

$$\chi^{-+}(\mathbf{q}, t) = i \frac{\mu_B g}{2\Omega} \Theta(t) \sum_{\mathbf{k}, \mathbf{k}'} \left\langle \left[c_{\mathbf{k}-\mathbf{q}\downarrow}^{\dagger}(t) c_{\mathbf{k}\uparrow}(t), c_{\mathbf{k}'+\mathbf{q}\uparrow}^{\dagger}(0) c_{\mathbf{k}'\downarrow}(0) \right] \right\rangle. \quad (24.12)$$

Diagrammatically, the susceptibility for noninteracting electrons can be represented as shown in Figure 24.5. The gray circles are spin vertices that require a spin-flip between incoming and outgoing spins, in the case of the transverse susceptibility χ^{-+} .

In the case of noninteracting electron systems, the definition of χ^{-+} in (24.12) clearly resembles Π_0 , the polarizability of the noninteracting electron gas, and we write

$$\chi_0^{-+}(\mathbf{q}, \omega) = -\frac{\mu_B g}{2\Omega} \Pi_0^{-+}(\mathbf{q}, \omega) = -\frac{\mu_B g}{2\Omega} \sum_{\mathbf{k}} \frac{n_{F\uparrow}(\varepsilon_{\mathbf{k}} - \mu) - n_{F\downarrow}(\varepsilon_{\mathbf{k}+\mathbf{q}} - \mu)}{\omega + \varepsilon_{\mathbf{k}} - \varepsilon_{\mathbf{k}+\mathbf{q}} + i\eta}. \quad (24.13)$$

In a manner similar to our treatment of the interacting electron gas, we use diagrammatic RPA techniques to derive expressions for the susceptibility in the present case. Typical RPA diagrams are shown in Figure 24.6: the RPA amounts to adding to the diagram 24.6(a) all possible interaction vertices of the form 24.6(b) that connect the two arms of the bubble to

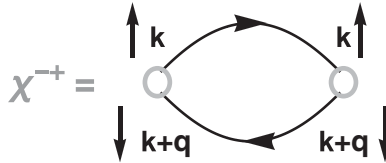


Figure 24.5 Diagrammatic representation of the transverse spin susceptibility χ^{-+} for noninteracting electrons.

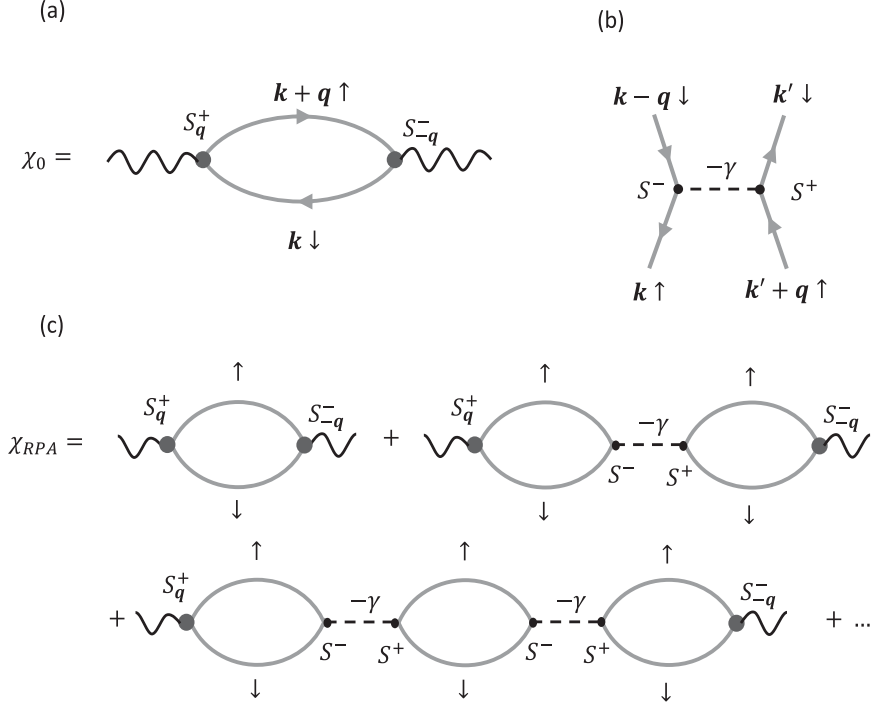


Figure 24.6 (a) Diagrammatic representation of the susceptibility χ_0^{-+} . (b) Diagrammatic representation of the interaction vertex, with strength γ . (c) The sum of bubble diagrams that gives the transverse spin susceptibility up to the RPA. Notice that the only way to connect the bare bubble is through an exchange vertex of the form presented in (b).

a consecutive bubble (as shown in 24.6(c)). If we now consider a local interaction, like the Hubbard model, $Un_{i\uparrow}n_{i\downarrow}$, $\gamma = U$, summing up this series, we get

$$\chi^{-+}(\mathbf{q}, \omega) = \frac{\chi_0^{-+}(\mathbf{q}, \omega)}{1 - U\chi_0^{-+}(\mathbf{q}, \omega)}.$$

Again, it is clear that an instability will occur if the condition $U\Pi_0^{-+}(\mathbf{q}, \omega) \geq 1$ is satisfied. This more general condition is satisfied for the ferromagnetic instability, when we take the limit $\Pi_0^{-+}(\mathbf{q} \rightarrow 0, 0) \rightarrow \mathcal{D}_{\uparrow}(\varepsilon_F)$, yielding the Stoner criterion $U\mathcal{D}(\varepsilon_F) \geq 1$.

24.2.2 Mean-Field Stoner Excitations

The mean-field approximation amounts to replacing the interacting system with an effective noninteracting system where the original noninteracting particle spectrum gets renormalized. In that spirit, we need to replace the denominator of (24.13) with corresponding terms from the Stoner mean-field spectrum of (24.3), namely,

$$\begin{aligned}
-\varepsilon_{\mathbf{k}} + \varepsilon_{\mathbf{k}+\mathbf{q}} &\rightarrow -\mathcal{E}_{\mathbf{k}\uparrow}^{\text{MF}} + \mathcal{E}_{\mathbf{k}+\mathbf{q}\downarrow}^{\text{MF}} = -\varepsilon_{\mathbf{k}} + \varepsilon_{\mathbf{k}+\mathbf{q}} - U\bar{n}(1-\zeta) + U\bar{n}(1+\zeta) \\
[2pt] &= \varepsilon_{\mathbf{k}+\mathbf{q}} - \varepsilon_{\mathbf{k}} + 2U\bar{n}\zeta \\
[2pt] &= \varepsilon_{\mathbf{k}+\mathbf{q}} - \varepsilon_{\mathbf{k}} + \Delta.
\end{aligned} \tag{24.14}$$

And we write the noninteracting Stoner magnetic susceptibility as

$$\chi_{0, \text{Stoner}}^{-+}(\mathbf{q}, \omega) = \frac{\mu_B g}{2\Omega} \sum_{\mathbf{k}} \frac{n_{F\uparrow}(\varepsilon_{\mathbf{k}} - \mu) - n_{F\downarrow}(\varepsilon_{\mathbf{k}+\mathbf{q}} - \mu)}{\omega - \varepsilon_{\mathbf{k}+\mathbf{q}} + \varepsilon_{\mathbf{k}} - \Delta + i\eta}. \tag{24.15}$$

The excitation energy of the noninteracting Stoner model is given by the poles of the Stoner susceptibility, as

$$\varepsilon_{\mathbf{k}+\mathbf{q}} - \varepsilon_{\mathbf{k}} + \Delta = \frac{\hbar^2}{m} \mathbf{k} \cdot \mathbf{q} + \frac{\hbar^2}{2m} q^2 + \Delta$$

depends on \mathbf{k} for a fixed $\mathbf{q} \neq 0$. Therefore, for any $\mathbf{q} \neq 0$ we find a continuum of electron-hole excitations, coined *Stoner particle-hole continuum* (see Figure 24.7). Only for $\mathbf{q} = 0$, the excitation energy is sharp, $\Delta = 2U\bar{n}\zeta > 0$. Excitations with vanishing energy exist when the two Fermi spheres above cross, as shown in Figure 24.8 since then we have at the crossing points

$$\varepsilon_{\mathbf{k}} - U\bar{n}\zeta = \mathcal{E}_F, \text{ and } \varepsilon_{\mathbf{k}+\mathbf{q}} + U\bar{n}\zeta = \mathcal{E}_F$$

and thus

$$\varepsilon_{\mathbf{k}+\mathbf{q}} - \varepsilon_{\mathbf{k}} + 2U\bar{n}\zeta = \varepsilon_{\mathbf{k}+\mathbf{q}} + U\bar{n}\zeta - (\varepsilon_{\mathbf{k}} - U\bar{n}\zeta) = \mathcal{E}_F - \mathcal{E}_F.$$

Zero-energy excitations are dangerous, since they suggest an instability of the mean-field ground state. One has to go beyond Stoner theory to see that they do not destroy the ferromagnetic ground state in this case.

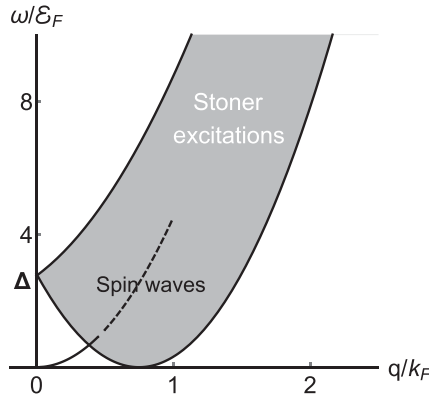


Figure 24.7 Stoner excitations spectrum.

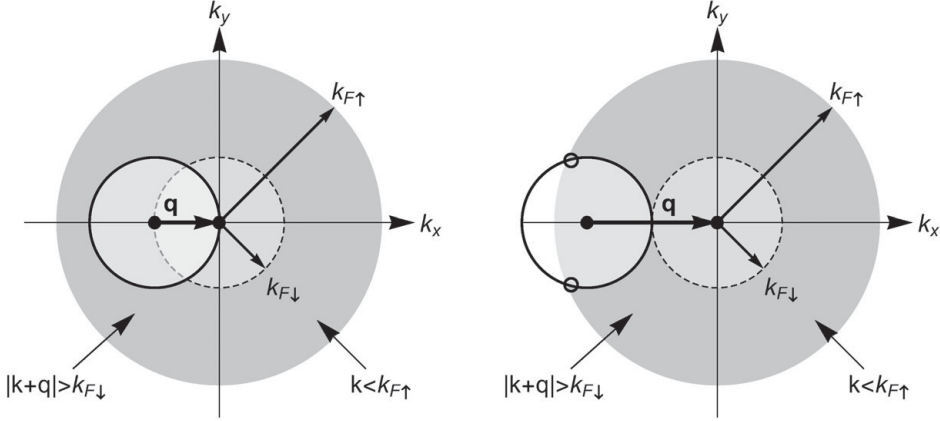


Figure 24.8 Relative disposition of the \uparrow and \downarrow Fermi seas at two different \mathbf{q} vectors. The black dots indicate zero energy excitations.

24.2.3 Susceptibility of Interacting System and Spin Waves

Following the RPA procedure, we can write the susceptibility of the interacting ferromagnetic system as

$$\chi^{-+}(\mathbf{q}, \omega) = \frac{\chi_{0, \text{Stoner}}^{-+}(\mathbf{q}, \omega)}{1 - U \chi_{0, \text{Stoner}}^{-+}(\mathbf{q}, \omega)}.$$

The poles of χ^{-+} determine the excitation spectrum of the itinerant ferromagnet with spin flipping. The poles equation becomes

$$1 - U \chi_{0, \text{Stoner}}(\mathbf{q}, \omega) = 0 \quad \Rightarrow \quad \chi_{0, \text{Stoner}}(\mathbf{q}, \omega) = \frac{1}{U}.$$

At $T = 0$, we get

$$\sum_{\mathbf{k}} \frac{\Theta(\mu - \varepsilon_{\mathbf{k}} + \gamma \zeta) [1 - \Theta(\varepsilon_{\mathbf{k}+\mathbf{q}} + \gamma \zeta - \mu)]}{\omega - \frac{\hbar^2}{m} \mathbf{k} \cdot \mathbf{q} - \frac{\hbar^2}{2m} q^2 - \Delta} = \frac{2\Omega}{\mu_B g U} = \frac{1}{V}. \quad (24.16)$$

We note that there are two types of singularities:

- For fixed \mathbf{q} , a series of poles fill the branch cut along the real ω -axis, between ω_{\min} and ω_{\max} . We note that there are as many intersections of the curves, associated with these poles, with the horizontal line $\chi_{0, \text{Stoner}}^{-+} = 1/U$. These give rise to the Stoner excitations.
- There is one intersection that lies at some ω below the quasicontinuum. At long wavelengths and $\omega \ll \Delta$, we have a new spin-wave excitation branch, reminiscent of plasmons, as indicated by the root $\omega_{\mathbf{q}}$ in Figure 24.9. Clearly, when $U \rightarrow 0$, $\omega_{\mathbf{q}} \rightarrow \omega_{\min}$ and the discrete state merges into the quasicontinuum. However, unlike plasmons, when

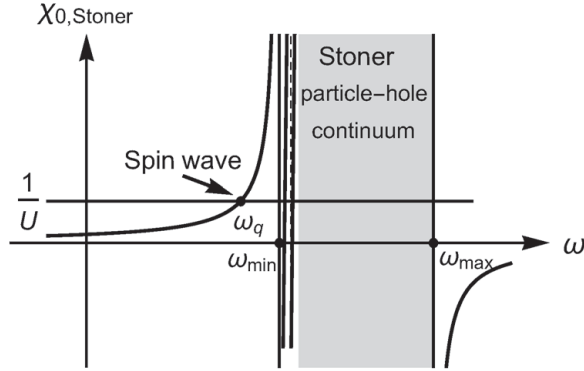


Figure 24.9 Extraction of spin-wave dispersion.

$\mathbf{q} = 0$, (24.16) shows that $\chi_{0, \text{Stoner}}^{-+} = 1/U$ has one root $\omega = \Delta + \frac{\mu_B g U}{2\Omega}$, so that the spin-wave frequency

$$\lim_{\mathbf{q} \rightarrow 0} \omega_{\mathbf{q}} = 0.$$

24.3 Nesting and Spin-Density Waves

We now explore instabilities that may possibly lead to magnetic orderings other than a uniform ferromagnetic phase in itinerant electronic systems. Such instabilities will be manifest as $\omega = 0$ singularities in the response function

$$\chi^{-+}(\mathbf{q}, 0) = \frac{\chi_{0, \text{Stoner}}^{-+}(\mathbf{q}, 0)}{1 - U\chi_{0, \text{Stoner}}^{-+}(\mathbf{q}, 0)} \Rightarrow 1 - U\chi_{0, \text{Stoner}}^{-+}(\mathbf{q}, 0) = 0$$

at some finite q , indicating a spatially varying magnetization. However, a \mathbf{q} wavevector instability is likely to develop if there exists a large region of the Fermi surface where $\varepsilon_{\mathbf{k}} = \varepsilon_{\mathbf{k}+\mathbf{q}}$ for some fixed vector \mathbf{q} , in a nesting fashion similar to the case of charge-density waves described in Chapter 7. As we have seen, in one dimension, the problem is particularly simple because we have natural nesting; and the instability occurs at $q = 2k_F$. In dimensions > 1 , such an instability relies on there being a part of the Fermi surface that is parallel to another part, so that a constant wavevector can connect particles and holes across the Fermi sea. Examples of how this may occur are shown in Figure 24.10; note that at half-filling, tight-binding band structures show the presence of nesting across the entire Fermi surface.

Spin-Density Waves versus AFM

The AFM behavior of a half-filled insulator can be regarded as a spatially varying magnetization. However, we should distinguish between such a phase and the presence of *spin-density waves*: the AFM phase displays strong sublattice polarization, in the sense

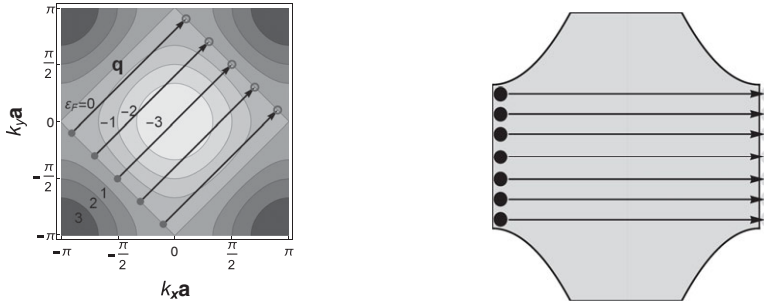


Figure 24.10 Right: half-filling, so $(\pi, \pi)/a_{\text{lattice}}$ wavevector generically leads to nesting. Left: Fermi surface in which a region is nested, so that the same spin-density-wave wavevector couples many points on the Fermi surface.

that each site had its entire magnetic moment points in some direction. By contrast, the *spin-density wave* scenario, which is the subject of this section, describes an instability that grows continuously from zero, and represents a small, partial magnetization at each site. It is however worth noticing that half-filling is a state particularly susceptible to spin-density wave ordering, and that with increasing interaction strength, there is a crossover from the spin-density wave ordering of a weakly interacting half-filled itinerant electron system to the AFM of a half-filled Mott insulator.

24.4 Anderson Model of Magnetic Impurities

The magnetic instabilities previously discussed mainly occur in metals with narrow bands, such as $3d$ -bands in the first row transition metals or f -bands in rare-earth metals and metal actinides.

Here we shall study the process of formation of local magnetic moments and the effect of substitutional magnetic impurities in a nonmagnetic host metal. When atoms of these magnetic metals are dissolved in nonmagnetic metallic hosts, they sometimes retain many features of magnetism, such as temperature-dependent susceptibility following a Curie-like behavior. Since such behavior cannot be explained by a one-electron model, it is obvious that interelectron interactions must play an essential role. We have studied the s - d exchange interaction, and derived the form of the long-range RKKY interaction among spins localized on different sites in a nonmagnetic metal, such as Mn in Cu. However, when elements of the iron group are introduced into a nonmagnetic metal, it is not always the case that they display a permanent magnetic moment. Fe and Mn in Cu maintain their spins, while Mn in Al does not. For the first case, we may use the s - d exchange interaction model. In the second case, one must understand why there is no magnetic moment on the transition ion impurity.

Another role of magnetic impurity atoms is revealed in the historic origin of the Kondo problem. This problem is interesting in showing a large separation of energy scales between

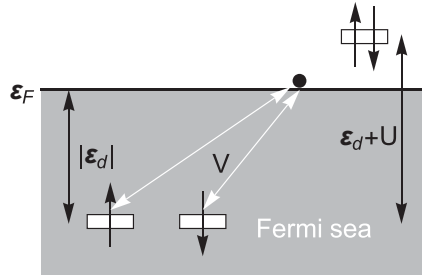


Figure 24.11 P. W. Anderson. Schematic of the Anderson magnetic impurity model.

the microscopic Hamiltonian and the effective binding energy of the ground state, hence producing a wide range of temperatures in which response properties are dominated by excited, rather than ground-state, configurations.

In order to study the conditions for an impurity to sustain a permanent magnetic moment, we require an approach where both cases can be explained with the same model. Such an approach is based on the Anderson model.

24.4.1 Anderson Hamiltonian and Local Moment Formation

Anderson realized that the moment formation has origins in strong correlations, which implies strong Coulomb interactions. Thus, in order to study the formation of localized magnetic states, Anderson proposed a model Hamiltonian [14], which turns out to be very closely related to the Hubbard Hamiltonian discussed earlier. As we have seen so far, Coulomb repulsion, specially onsite between antiparallel spins, tends to localize electrons. In contrast, Anderson also recognized that localized atomic orbitals are amenable to tunneling into free electronic states, as shown in Figure 24.11, when their atomic energy level overlaps with the free electron band.

The Anderson Hamiltonian depicts a model of localized states, represented by the operators¹ d^\dagger , d , coupled to delocalized conduction electrons. Because of their spatial confinement, the localized states have a strong Hubbard U , which justifies the neglect of the much weaker repulsive interaction between conduction electrons. The Hamiltonian is written as

$$\mathcal{H}_A = \sum_{\mathbf{k}\sigma} \varepsilon_{\mathbf{k}\sigma} c_{\mathbf{k}\sigma}^\dagger c_{\mathbf{k}\sigma} + \varepsilon_d \sum_{\sigma} d_{\sigma}^\dagger d_{\sigma} + U d_{\uparrow}^\dagger d_{\uparrow} d_{\downarrow}^\dagger d_{\downarrow} + \frac{V}{\sqrt{\Omega}} \sum_{\mathbf{k}\sigma} \left[d_{\sigma}^\dagger c_{\mathbf{k}\sigma} + c_{\mathbf{k}\sigma}^\dagger d_{\sigma} \right].$$

The impurity spin operator can be written as

$$\mathbf{S} = \frac{1}{2} \sum_{\sigma\sigma'} d_{\sigma}^\dagger \boldsymbol{\tau}_{\sigma\sigma'} d_{\sigma'},$$

¹ Although we are using the symbol d to denote creation and annihilation operators associated with the localized orbital, the orbital may be of d or f type. Similarly, we shall use ε_d to denote the orbital energy.

where τ is the Pauli matrix. We write

$$\mathbf{S} \cdot \mathbf{S} = \frac{5}{4} (n_{d\uparrow} + n_{d\downarrow}) + \frac{3}{4} n_{d\uparrow} n_{d\downarrow}$$

so that the impurity Hamiltonian can be written as

$$\mathcal{H}_d = \sum_{\mathbf{k}\sigma} \left(\varepsilon_{\mathbf{k}\sigma} + \frac{5}{3} U \right) c_{\mathbf{k}\sigma}^\dagger c_{\mathbf{k}\sigma} - \frac{4}{3} U \mathbf{S} \cdot \mathbf{S}.$$

Thus, if U is “large enough,” and if we can arrange things such that $\langle n_d \rangle \neq 0$, the impurity will maximize $\mathbf{S} \cdot \mathbf{S}$, and will acquire a moment!

First, we shall determine the conditions required for the single occupation of the localized level, namely, one electron, rather than zero or two. Second, we shall investigate when this localized magnetic moment remains free, rather than being screened by spin fluctuations of the surrounding Fermi sea.

It is important to note the energy scales of these two different processes; the interesting physics is that two very different energy scales arise from these two problems.

Virtual Bound-State Formation and Hybridization Resonance

In order to separate the different competing mechanisms contained in the Anderson Hamiltonian, we will turn off the interaction U and consider hybridization effects only. The effect is manifest in a narrow resonance induced by the impurity, which is essentially an atomic level broadened by the hybridization with the conduction electrons of the host metal.

We shall examine here the ensuing resonant scattering off a noninteracting d/f -level, using the Green function approach.

Impurity Green Function

The localized retarded Green function G_d is given by

$$G_d(t) = -i\Theta(t) \left\langle \left[d_\sigma(t), d_\sigma^\dagger(0) \right] \right\rangle.$$

The equation of motion is

$$\begin{aligned} \frac{\partial G_d}{\partial t} &= -i\delta(t) \left\langle \left[d_\sigma(t), d_\sigma^\dagger(0) \right] \right\rangle - i\Theta(t) \left\langle \left[\frac{\partial d_\sigma(t)}{\partial t}, d_\sigma^\dagger(0) \right] \right\rangle \\ i \frac{\partial G_d}{\partial t} &= \delta(t) - i\Theta(t) \left\langle \left[[d_\sigma(t), \mathcal{H}], d_\sigma^\dagger(0) \right] \right\rangle. \end{aligned} \quad (24.17)$$

The commutator couples G_d to a mixed propagator

$$G_{\mathbf{k}d}(t) = -i\Theta(t) \left\langle \left[c_{\mathbf{k}\sigma}^\dagger(t), d_\sigma^\dagger(0) \right] \right\rangle$$

according to the equation

$$i \frac{\partial G_d}{\partial t} = \delta(t) + \varepsilon_d G_d + \sum_{\mathbf{k}} V G_{\mathbf{k}d}(t) \quad \Rightarrow \quad (\omega - \varepsilon_d) G_d(\omega) = 1 + \sum_{\mathbf{k}} V G_{\mathbf{k}d}(\omega).$$

We find in the same way that

$$(\omega - \varepsilon_{\mathbf{k}}) G_{\mathbf{k}d}(\omega) - V G_d(\omega) = 0.$$

Eliminating $G_{\mathbf{k}d}$, we finally have

$$G_d(\omega) = \frac{1}{\omega - \varepsilon_d - \Sigma(d, \omega)} = \frac{1}{G_d^{(0)-1} - \Sigma(d, \omega)}$$

$$\Sigma(d, \omega + i\eta) = \sum_{\mathbf{k}} \frac{V^2}{\omega - \varepsilon_{\mathbf{k}} + i\eta}.$$

We represent the propagator of the bare d/f -electron by a black line, and that of the conduction electron by a gray line:

$$G_d^{(0)}(\omega) = \frac{1}{\omega - \varepsilon_d}, \quad \text{---} \xrightarrow{\text{d}, \omega}$$

$$G_{\mathbf{k}}^{(0)}(\omega) = \frac{1}{\omega - \varepsilon_{\mathbf{k}}}, \quad \text{---} \xrightarrow{\mathbf{k}, \omega}$$

The hybridization enables the d/f -electron to tunnel back and forth into the continuum, with a manifest *self-energy* diagram:

$$\text{---} \xrightarrow{\text{d}, \omega} \text{---} \xrightarrow{\mathbf{k}, \omega} \text{---} \xrightarrow{\text{d}, \omega} \text{---} = \Sigma(d, \omega) = \sum_{\mathbf{k}} \frac{V^2}{\omega - \varepsilon_{\mathbf{k}} + i\eta},$$

where we have assumed a \mathbf{k} -independent (contact scattering) hybridization interaction. This diagram can also be considered as an effective retarded (frequency/time-dependent) scattering potential for d/f -electrons, since the electron can spend significant time in the conduction band. The multiple scattering processes of the d/f -electron are represented by

$$\text{---} \xrightarrow{\text{d}} \text{---} \xrightarrow{\mathbf{k}', \omega} \text{---} \xrightarrow{\mathbf{k}', \omega} \text{---} \xrightarrow{\mathbf{k}'', \omega} \text{---} \xrightarrow{\mathbf{k}'', \omega} \text{---}$$

We note that the electron assumes a different momentum each time it tunnels into the conduction band, and we have to sum over all possible values of these intermediate state momenta available in the conduction band.

We assume a broad conduction band of width $[-W, W]$, and we calculate $\Sigma(d, \omega \pm i\eta)$ as

$$\Sigma(d, \omega + i\eta) = \int \frac{d\varepsilon}{\pi} \mathcal{D}(\varepsilon) \frac{\pi V^2}{\omega - \varepsilon + i\eta} = \int \frac{d\varepsilon}{\pi} \frac{\Delta(\varepsilon)}{\omega - \varepsilon + i\eta},$$

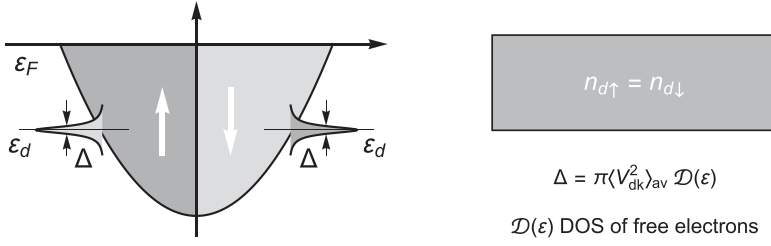


Figure 24.12 Resonance in the absence of Coulomb interactions. No localized moments.

where $\mathcal{D}(\varepsilon)$ is the DOS of the conduction band, and $\Delta(\varepsilon) = \pi \mathcal{D}_c(\varepsilon) V^2$. We further simplify the problem by assuming a uniform DOS, such that $\Delta(\varepsilon) = \Delta$, and obtain

$$\begin{aligned} \Sigma(\omega + i\eta) &= \frac{\Delta}{\pi} \int_{-W}^W \frac{d\varepsilon}{\omega - \varepsilon + i\eta} = \frac{\Delta}{\pi} \left(\text{P} \int_{-W}^W \frac{d\varepsilon}{\omega - \varepsilon} - i\pi \Theta(W - |\omega|) \right) \\ &= -\frac{\Delta}{\pi} \ln \left[\frac{\omega + W}{\omega - W} \right] - i\Delta \Theta(W - |\omega|). \end{aligned}$$

$\text{Re } \Sigma_c$ is of order $O(\omega/W)$, which for $\Delta \ll W$ is negligible. Consequently, we obtain the simple form of the d , f -propagator

$$G_d(\omega) = \frac{1}{\omega - \varepsilon_d - i\Delta}.$$

It describes a resonance of width Δ , centered around ε_d , as shown in Figure 24.12, with a density of states


$$\mathcal{D}_d(\omega) = \frac{1}{\pi} \text{Im } G_d(\omega - \varepsilon_d - i\eta) = \frac{\Delta}{(\omega - \varepsilon_d)^2 + \Delta^2}.$$

Conduction Electrons Green Function

Next we consider this multiple scattering process from the perspective of the conduction electrons, where we reverse the roles of the propagators, and write

$$\text{Diagram (24.18): } k \rightarrow k' \rightarrow k \rightarrow k' \rightarrow k \rightarrow k'' \rightarrow k' \quad (24.18)$$

First, note that the presence of the impurity breaks the translation symmetry of the Hamiltonian, and $G(\mathbf{k}', \mathbf{k}; \omega)$ is no longer diagonal in the momentum variables. Moreover, we note that the multiple scattering from the impurity can be cast in terms of a \mathcal{T} -matrix, which contains the shaded areas in (24.18), and similar diagrams in higher terms – this yields precisely $V^2 G_d$. Consequently, we represent the full (broadened) d , f -propagator by



$$\begin{aligned}
 G(\mathbf{k}', \mathbf{k}; \omega) &= \delta_{\mathbf{k}\mathbf{k}'} G^{(0)}(\mathbf{k}, \omega) + G^{(0)}(\mathbf{k}, \omega) V^2 G_d(\omega) G^{(0)}(\mathbf{k}', \omega) \\
 &= \delta_{\mathbf{k}\mathbf{k}'} G^{(0)}(\mathbf{k}, \omega) + G^{(0)}(\mathbf{k}, \omega) \mathcal{T}(\omega) G^{(0)}(\mathbf{k}', \omega).
 \end{aligned} \quad (24.19)$$

We write the \mathcal{T} -matrix as

$$\mathcal{T}(\omega) \equiv V^2 G_d(\omega) = \frac{1}{\pi \mathcal{D}(\omega)} \frac{\Delta}{\omega - \varepsilon_d + i\Delta} = -\frac{1}{\pi \mathcal{D}(\omega)} \frac{1}{\frac{\varepsilon_d - \omega}{\Delta} - i}. \quad (24.20)$$

Scattering Phase Shift and Friedel Sum Rule

We recall from scattering theory that the \mathcal{S} -matrix can be expressed as

$$\mathcal{S}(\omega) = e^{2i\delta(\omega)} = 1 - 2\pi i \mathcal{D}(\omega) \mathcal{T}(\omega + i\eta),$$

where $\delta(\omega)$ is the scattering phase shift, so that

$$\mathcal{T}(\omega + i\eta) = \frac{1}{2i\pi \mathcal{D}(\omega)} [\mathcal{S}(\omega) - 1] = -\frac{1}{\pi \mathcal{D}(\omega)} \frac{1}{\cot[\delta(\omega)] - i}. \quad (24.21)$$

From (24.20) and (24.21), we obtain the scattering phase shift

$$\delta_d(\omega) = \cot^{-1} \left(\frac{\varepsilon_d - \omega}{\Delta} \right).$$

$\delta_d(\omega)$ increases from $\delta_d(\omega \ll \varepsilon_d) \sim 0$ to $\delta_d(\omega \gg \varepsilon_d) = \pi$; at resonance, $\delta(\varepsilon_d) = \pi/2$.

The Anderson model provides a microscopic manifestation of the Friedel sum rule, which relates the phase shifts of the conduction electrons scattered on the impurity to the number of displaced electrons.

Friedel Sum Rule

Friedel considered the presence of a localized impurity in a host metal [68]. We recall from quantum mechanics that the scattering wavefunction can be written as

$$\Psi(\mathbf{x}) = \frac{1}{k} \sum_l (2l+1) i^l e^{i\delta_l} P_l(\cos \theta) \psi_l(r).$$

Setting $\psi_l = \varphi_l/r$, and taking spin degeneracy into account, we obtain the total electron number within a sphere of radius R as

$$\begin{aligned}
 4\pi \int_0^R dr r^2 n(r) &= 4\pi \int_0^R dr r^2 2 \int_0^{k_F} 4\pi dk k^2 \frac{1}{(2\pi)^3} \sum_l (2l+1) \frac{\psi_l^2(r)}{k^2} \\
 &= \frac{4}{\pi} \sum_l (2l+1) \int_0^{k_F} dk \int_0^R dr \varphi_l^2(r).
 \end{aligned}$$

The Schrödinger equation for φ_l is given by

$$\begin{cases} \frac{d^2 \varphi_l}{dr^2} + \left[k^2 - \frac{l(l+1)}{r^2} - \frac{2mV(r)}{\hbar^2} \right] \varphi_l = 0 \\ \frac{d^2 \bar{\varphi}_l}{dr^2} + \left[\bar{k}^2 - \frac{l(l+1)}{r^2} - \frac{2mV(r)}{\hbar^2} \right] \bar{\varphi}_l = 0 \end{cases}$$

From these two equations, we obtain

$$(\bar{k}^2 - k^2) \int_0^R dr \bar{\varphi} \varphi = \int_0^R dr \left[\bar{\varphi} \frac{d^2 \varphi}{dr^2} - \varphi \frac{d^2 \bar{\varphi}}{dr^2} \right] = \left[\bar{\varphi} \frac{d\varphi}{dr} - \varphi \frac{d\bar{\varphi}}{dr} \right]_0^R.$$

which in the limit $\bar{k} \rightarrow k$ yields

$$\int_0^R dr \varphi_l^2(r) = \frac{1}{2k} \left[\frac{d\varphi}{dk} \frac{d\varphi}{dr} - \varphi \frac{d^2 \varphi}{dr dk} \right]_{r=R}.$$

Using the asymptotic form of φ

$$\varphi(R) \simeq \sin \left(kR + \delta_l(k) - \frac{l\pi}{2} \right),$$

we obtain

$$\int_0^R dr r^2 n(r) = \frac{2}{\pi} \sum_l (2l+1) \int_0^{k_F} dk \left[\left(R + \frac{d\delta_l}{dk} \right) - \frac{1}{2k} \sin(2kR + 2\delta_l(k) - l\pi) \right].$$

The change in electron number is given by

$$\begin{aligned} \Delta N &= \int_0^R (n(r) - n_0(r)) 4\pi r^2 dr \\ &= \frac{2}{\pi} \sum_l (2l+1) \int_0^{k_F} dk \left[\left(\frac{d\delta_l}{dk} \right) - \frac{1}{k} \sin \delta_l(k) \cos(2kR + \delta_l(k) - l\pi) \right]. \end{aligned}$$

Considering the weak k -dependence of $\delta_l(k)$ compared to $2kR$, and partially integrating, we obtain

$$\Delta N = \frac{2}{\pi} \sum_l (2l+1) \left[\delta_l(k_F) - \frac{1}{2k_F R} \sin \delta_l(k_F) \sin(2k_F R + \delta_l(k_F) - l\pi) \right].$$

In the limit $R \rightarrow \infty$, we should obtain the density difference between the impurity and the host, namely

$$\Delta n = \frac{2}{\pi} \sum_l (2l+1) \delta_l(k_F).$$

Thus we surmise that the phase shift $\delta_d = \delta_d(\varepsilon_F = 0)$ at the Fermi surface determines the amount of charge bound inside the resonance. We can determine this charge by using the d/f -spectral function to calculate the ground-state occupancy:

$$n_d = \int_{-\infty}^0 d\omega \mathcal{D}(\omega) = 2 \int_{-\infty}^0 \frac{d\omega}{\pi} \frac{\Delta}{(\omega - \varepsilon_d)^2 + \Delta^2} = \frac{2}{\pi} \cot^{-1} \left(\frac{\varepsilon_d}{\Delta} \right) = \frac{\delta_d}{\pi/2}. \quad (24.22)$$

Note that when $\delta_d(0) = \pi/2$, $n_d = 1$. This is a particular example of the *Friedel sum rule*.

24.4.2 Hartree–Fock Physics of the Anderson Model

The Anderson model presents a competition between the Coulomb interaction and hybridization. We would expect that local moments will develop when the Coulomb interaction exceeds the hybridization – the question is how can we quantify this. For $U \neq 0$, we rewrite (24.17) in the form

$$\begin{aligned} i \frac{\partial G_{d\sigma}}{\partial t} &= \delta(t) - i\Theta(t) \left\langle \left[[d_\sigma(t), \mathcal{H}], d_\sigma^\dagger(0) \right] \right\rangle \\ &= \delta(t) + \varepsilon_d G_{d\sigma}(t) + V \sum_{\mathbf{k}} G_{\mathbf{k}d\sigma}(t) - i\Theta(t) U \left\langle \left[d_\sigma(t) n_{\bar{\sigma}}(t), d_\sigma^\dagger(0) \right] \right\rangle \end{aligned}$$

and we find that the right-hand side contains a higher-order Green function that eventually leads to an infinite hierarchy of equations. We can avoid this complication by applying the Hartree–Fock approximation to terminate the hierarchy and simplify the problem. This amounts to neglecting the correlations between the “up” and “down” electron in the impurity orbital, namely,

$$n_{\bar{\sigma}}(t) = (n_{\bar{\sigma}}(t) - \langle n_{\bar{\sigma}} \rangle) + \langle n_{\bar{\sigma}} \rangle \simeq \langle n_{\bar{\sigma}} \rangle.$$

The validity of the Hartree–Fock solution would require that the correlation time scale $1/U$ be much larger than the lifetime of the localized state $1/\Delta$. This translates to $\Delta \gg U$, which may not apply in the magnetic regime!

However, to gain an initial insight into the effect of hybridization on local moment formation, Anderson originally developed following Hartree–Fock mean-field treatment: first, we modify the impurity Green function, to read

$$G_{d\sigma}(\omega) = \frac{1}{\omega - \varepsilon_d - U \langle n_{\bar{\sigma}} \rangle - i\Delta},$$

which means that we set

$$\begin{aligned} \varepsilon_d &\rightarrow E_{d\sigma} = \varepsilon_d + U \langle n_{\bar{\sigma}} \rangle \\ \langle n_{d\sigma} \rangle &= \frac{\delta_{d\sigma}}{\pi} = \frac{1}{\pi} \cot^{-1} \left(\frac{\varepsilon_d + U \langle n_{\bar{\sigma}} \rangle}{\Delta} \right). \end{aligned}$$

Anticipating that the development of a magnetic moment amounts to $\langle n_{d\uparrow} \rangle \neq \langle n_{d\downarrow} \rangle$, we introduce the following definitions:

$$\text{Total occupancy} \quad n_d = \sum_{\sigma} \langle n_{d\sigma} \rangle$$

$$\text{Magnetization} \quad \mu = \langle n_{\uparrow} \rangle - \langle n_{\downarrow} \rangle$$

$$\langle n_{d\sigma} \rangle = \frac{1}{2} (n_d + \sigma \mu), \quad \sigma = \pm 1$$

The self-consistent mean-field equation for occupancy and magnetization become

$$n_d = \frac{1}{\pi} \sum_{\sigma=\pm 1} \cot^{-1} \left(\frac{\varepsilon_d + (U/2) (n_d - \sigma \mu)}{\Delta} \right) \quad (24.23)$$

$$\mu = \frac{1}{\pi} \sum_{\sigma=\pm 1} \sigma \cot^{-1} \left(\frac{\varepsilon_d + (U/2) (n_d - \sigma \mu)}{\Delta} \right). \quad (24.24)$$

To obtain the critical interaction strength U_c , which defines the threshold for local moment formation, we set $\mu = 0$ in (24.23), yielding

$$\frac{\varepsilon_d + (U_c/2) n_d}{\Delta} = \cot \left(\frac{\pi n_d}{2} \right).$$

However, to ensure that we are taking the limit $\mu \rightarrow 0$, we take the derivative of (24.24) with respect to μ and then set $\mu = 0$; we obtain²

$$1 = \frac{U_c}{\pi \Delta} \frac{1}{1 + \left(\frac{\varepsilon_d + (U_c/2) n_d}{\Delta} \right)^2} = \frac{U_c}{\pi \Delta} \sin^2 \left(\frac{\pi n_d}{2} \right)$$

so that for a local moment to exist, namely, $n_d = 1$, we obtain

$$U_c = \pi \Delta.$$

For $U > U_c$, there are two solutions, corresponding to an “up” or “down” spin polarization of the d/f -state. We will see that this is an oversimplified description of the local moment, but it gives us an approximate picture of the physics. The total density of states now contains two Lorentzian peaks, located at $\varepsilon_d \pm M$:

$$\mathcal{D}_d(\omega) = \frac{1}{\pi} \left[\frac{\Delta}{(\omega - \varepsilon_d - UM)^2 + \Delta^2} + \frac{\Delta}{(\omega - \varepsilon_d + UM)^2 + \Delta^2} \right].$$

The critical curve obtained by plotting U_c and ε_d as a parametric function of n_d is shown in Figure 24.13.

The Anderson mean-field theory allows a qualitative understanding of the experimentally observed formation of local moments. When dilute magnetic ions are dissolved in a

² $\frac{d \cot^{-1}(x)}{dx} = \frac{1}{1+x^2}.$

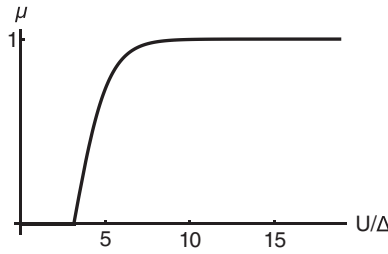


Figure 24.13 Mean-field magnetic moment.

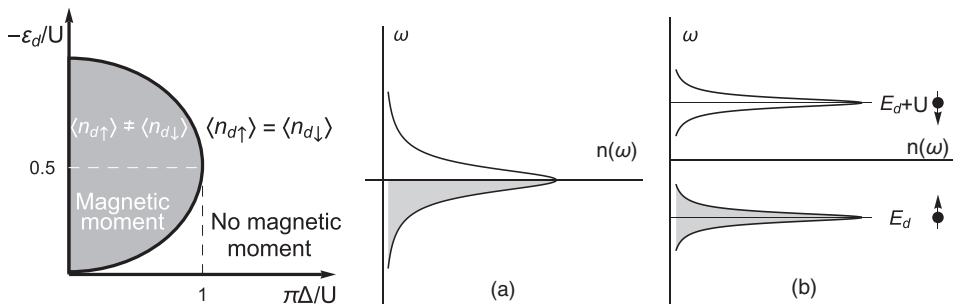


Figure 24.14 Mean-field phase diagram of the Anderson model, illustrating how the d , f -electron resonance splits to form a local moment. (a) $U < \pi \Delta$, single half-filled resonance. (b) $U > \pi \Delta$, up and down components of the resonance are split by an energy U .

metal to form an alloy, the formation of a local moment is dependent on whether the ratio $U/\pi \Delta$ is larger than or smaller than unity. When iron is dissolved in pure niobium, the failure of the moment to form reflects the higher density of states and larger value of Δ in this alloy. When iron is dissolved in molybdenum, the lower density of states causes $U > U_c$, and local moments form.

The case in which a magnetic moment can arise, as illustrated in Figure 24.14, is when the localized level has energy less than the Fermi level, so it will be occupied by at least one electron, but the interaction strength is large enough that the energy to have two electrons is greater than the Fermi level, i.e., $\varepsilon_d < \varepsilon_F < \varepsilon_d + U$.

The singly occupied impurity ground state is given by

$$|d_\sigma^1\rangle = d_\sigma^\dagger \prod_{\mathbf{k}}^{k_F} c_{\mathbf{k}\uparrow}^\dagger c_{\mathbf{k}\downarrow}^\dagger |0\rangle.$$

For simplicity, we also assume that excitations to

$$|d^2\rangle = d_\sigma^\dagger c_{\mathbf{k}\bar{\sigma}} |d_\sigma^1\rangle, \quad \text{or} \quad |d^0\rangle = c_{\mathbf{k}\sigma}^\dagger d_\sigma |d_\sigma^1\rangle,$$

i.e., respectively adding an electron to or removing an electron from the impurity cost the same amount of energy $U/2$. As a result, the situation becomes electron–hole symmetric: there are two Hubbard bands at the same energy that are each other’s mirror image through electron–hole inversion. Effectively, the impurity is now a localized $S = 1/2$ system that can switch its magnetization through either of two virtual processes, each with a transition rate $2V^2/U$:

$$\begin{aligned} |d_{\bar{\sigma}}^1\rangle &= c_{\mathbf{k}'\sigma}^\dagger d_{\sigma} d_{\bar{\sigma}}^\dagger c_{\mathbf{k}\bar{\sigma}} |d_{\sigma}^1\rangle && \text{via } |d^2\rangle \\ |d_{\sigma}^1\rangle &= d_{\bar{\sigma}}^\dagger c_{\mathbf{k}'\bar{\sigma}}^\dagger c_{\mathbf{k}\sigma}^\dagger d_{\sigma} |d_{\sigma}^1\rangle && \text{via } |d^0\rangle. \end{aligned}$$

We note that in this simple Hartree–Fock approach, we have a state consisting of a singly occupied d/f -state plus a filled Fermi sea: as shown in Figure 24.15, the occupancy is either $\langle n_{d\uparrow} \rangle = 1, \langle n_{d\downarrow} \rangle = 0$, or $\langle n_{d\downarrow} \rangle = 1, \langle n_{d\uparrow} \rangle = 0$, accounting for the two degenerate situations. We recall from the Friedel sum rule that the phase shift $\delta(\epsilon_F)$ divided by π gives the total number of occupying electrons. Thus for this doublet case, we have $\delta_{\uparrow} = \pi, \delta_{\downarrow} = 0$ or $\delta_{\uparrow} = 0, \delta_{\downarrow} = \pi$, as shown in Figure 24.16.

The question we turn to now is that of the ultimate fate of a local moment immersed in a sea of conduction electrons. In the large U limit, that is the limit in which the onsite repulsion energy U is much greater than the local moment resonance width Δ , we will examine the residual interaction between the local moment and the conduction electrons.

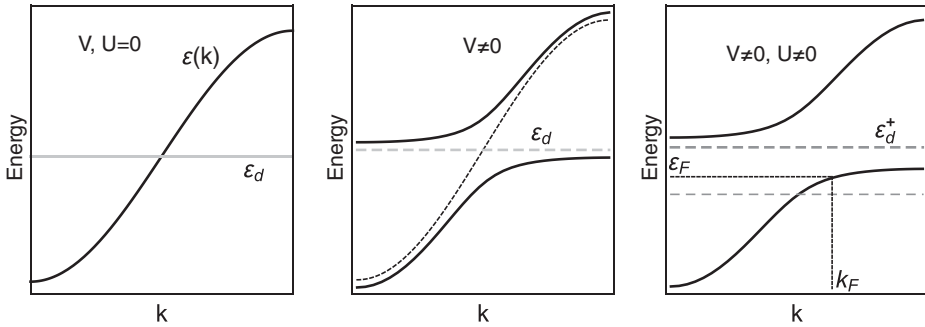


Figure 24.15 Electron dispersions: left $U = V = 0$; middle $V \neq 0, U = 0$; right $U, V \neq 0$. ϵ_d is the singly occupied d/f energy level, while $\epsilon_d + U$ is the doubly occupied level.

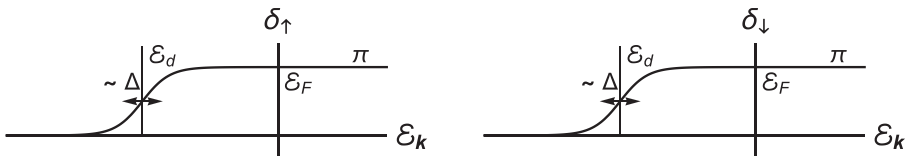


Figure 24.16 The impurity scattering phase shift for the conduction band states, reflecting single-occupancy in the mean-field state.

24.4.3 Relating the Anderson and Kondo Models: Schrieffer–Wolff Transformation

We understand now that in the regime $\Delta \ll |\varepsilon_d|$, $\varepsilon_d \ll \varepsilon_F \equiv 0$, and $\varepsilon_d + U > 0$, the energies of the empty and double occupied state, $|d^0\rangle$ and $|d^2\rangle$, lie above the $|d^1\rangle$ states, and they can be neglected at low temperatures – a local moment represented by a spin-1/2 is formed. This implies that local charge fluctuations on the d -level are suppressed at low temperatures, and only virtual exchange with conduction band electrons survive, leading to spin-flip processes. In other words, in systems that display an impurity moment, we surmise that the prerequisite of large $V \ll U$ means suppressing charge (or occupancy) fluctuations on the impurity, thus effectively quenching the impurity *charge degree of freedom*. The only degree of freedom that remains at the impurity is its spin, which carries low-energy spin excitations. For such systems, we write the Anderson Hamiltonian as

$$\begin{aligned}\mathcal{H}_A &= \mathcal{H}_0 + \mathcal{H}_h \\ \mathcal{H}_0 &= \sum_{\mathbf{k}\sigma} \varepsilon_{\mathbf{k}\sigma} c_{\mathbf{k}\sigma}^\dagger c_{\mathbf{k}\sigma} + \varepsilon_d \sum_{\sigma} d_{\sigma}^\dagger d_{\sigma} + U d_{\uparrow}^\dagger d_{\uparrow} d_{\downarrow}^\dagger d_{\downarrow} \\ \mathcal{H}_h &= \frac{V}{\sqrt{\Omega}} \left(d_{\sigma}^\dagger c_{\mathbf{k}\sigma} + \text{H.c.} \right),\end{aligned}$$

where we treat \mathcal{H}_h as a perturbation. We conjure the scenario where an electron that is strongly localized at the impurity may occasionally hop into the band, or a band electron hops on to the impurity site to gain kinetic energy. From our previous discussions, we infer that this leads to an antiferromagnetic exchange interaction between the local impurity spin and the conduction electron spin at the impurity site.

In 1966, Schrieffer and Wolff [162] proposed a scheme whereby the Anderson Hamiltonian is transformed into an effective one that supports the prescribed low-energy scenario. Following their approach, we consider an effective Hamiltonian restricted to the subspace in which the localized level is singly occupied.

We now follow the prescription proposed by Schrieffer and Wolff that involves the application of a canonical transformation of the form $e^{iS} \mathcal{H} e^{-iS} = \tilde{\mathcal{H}}$. In the general scheme of the Schrieffer–Wolff transformation and within the restricted Hilbert space, we begin by partitioning \mathcal{H}_h into components that effect transitions between Hilbert subspaces with different occupancies, as shown in Figure 24.17,

$$\begin{aligned}\mathcal{H}_h &= \frac{V}{\sqrt{\Omega}} \sum_{\mathbf{k}} [\mathcal{H}_{21}(\mathbf{k}) + \mathcal{H}_{12}(\mathbf{k}) + \mathcal{H}_{01}(\mathbf{k}) + \mathcal{H}_{10}(\mathbf{k})] \\ \mathcal{H}_{12}(\mathbf{k}) &= \sum_{\sigma} n_{\bar{\sigma}} d_{\sigma}^\dagger c_{\mathbf{k}\sigma}, \quad \mathcal{H}_{10}(\mathbf{k}) = \sum_{\sigma} (1 - n_{\bar{\sigma}}) c_{\mathbf{k}\sigma}^\dagger d_{\sigma},\end{aligned}$$

where $n \equiv n_d$ is the population of the d level. We note that \mathcal{H}_{12} takes the localized state from singly occupied to doubly occupied, $n_d = 1 \rightarrow 2$, and \mathcal{H}_{10} takes it from singly occupied to empty. The presence of $n_{\bar{\sigma}}$ in \mathcal{H}_{12} and $1 - n_{\bar{\sigma}}$ in \mathcal{H}_{10} ensures that the impurity level is already singly occupied. \mathcal{H}_{21} , \mathcal{H}_{01} are the appropriate Hermitian conjugates.

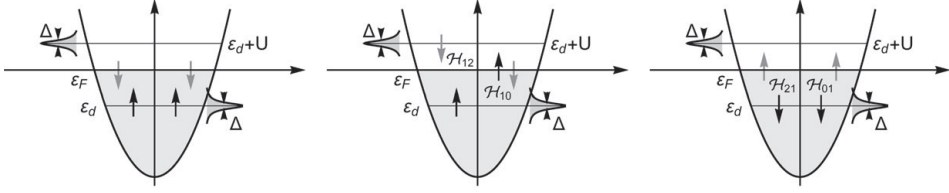


Figure 24.17 Virtual spin-flip transitions under impurity single-occupancy constraint.

At this point, we should be familiar with the application of this type of canonical transformation. We expand to second order

$$\tilde{\mathcal{H}} = \mathcal{H}_0 + i [S, \mathcal{H}_0] + \mathcal{H}_h + i [S, \mathcal{H}_h] - \frac{1}{2} [S, [S, \mathcal{H}_0]] + \dots$$

and require that $[S, \mathcal{H}_0] = i\mathcal{H}_h$. We then arrive at

$$\tilde{\mathcal{H}} = \mathcal{H}_0 + \frac{i}{2} [S, \mathcal{H}_h].$$

To determine S , we note that

$$\begin{aligned} [\mathcal{H}_{12}(\mathbf{k}), \mathcal{H}_0] &= (\varepsilon_{\mathbf{k}} - \varepsilon_d - U) \sum_{\sigma} n_{\bar{\sigma}} d^{\dagger} c_{\mathbf{k}\sigma} \\ [\mathcal{H}_{10}(\mathbf{k}), \mathcal{H}_0] &= -(\varepsilon_{\mathbf{k}} - \varepsilon_d) \sum_{\sigma} (1 - n_{\bar{\sigma}}) c_{\mathbf{k}\sigma}^{\dagger} d_{\sigma}. \end{aligned}$$

The energy prefactors represent the difference between before and after the application of the corresponding \mathcal{H}_h operator. The Hermitian conjugate terms should have opposite signs. We obtain

$$S = i \frac{V}{\sqrt{\Omega}} \sum_{\mathbf{k}} \left[\frac{\mathcal{H}_{21}(\mathbf{k}) - \mathcal{H}_{12}(\mathbf{k})}{\varepsilon_{\mathbf{k}} - \varepsilon_d - U} - \frac{\mathcal{H}_{10}(\mathbf{k}) - \mathcal{H}_{01}(\mathbf{k})}{\varepsilon_{\mathbf{k}} - \varepsilon_d} \right]. \quad (24.25)$$

In the expansion of $[S, \mathcal{H}_h]$, we only retain terms pertinent to the Hilbert subspace of single occupancy, namely terms like $\mathcal{H}_{12}(\mathbf{k})\mathcal{H}_{21}(\mathbf{k})$ and $\mathcal{H}_{10}(\mathbf{k})\mathcal{H}_{01}(\mathbf{k})$, which represent virtual double or single occupancy. We thus obtain

$$\begin{aligned} \frac{i}{2} [S, \mathcal{H}_h] &\approx -\frac{V^2}{2\Omega} \sum_{\mathbf{k}\mathbf{k}'} \left[-\frac{\mathcal{H}_{12}(\mathbf{k})\mathcal{H}_{21}(\mathbf{k}') + \mathcal{H}_{12}(\mathbf{k}')\mathcal{H}_{21}(\mathbf{k})}{\varepsilon_{\mathbf{k}} - \varepsilon_d - U} \right. \\ &\quad \left. + \frac{\mathcal{H}_{10}(\mathbf{k})\mathcal{H}_{01}(\mathbf{k}') + \mathcal{H}_{10}(\mathbf{k}')\mathcal{H}_{01}(\mathbf{k})}{\varepsilon_{\mathbf{k}} - \varepsilon_d} \right]. \end{aligned} \quad (24.26)$$

Note the opposite signs coming from the opposite signs of \mathcal{H}_{21} and \mathcal{H}_{10} in (24.25).

To simplify the procedure, we invoke the assumption that the \mathbf{k} -dependence of the denominators is slow, which is justified when ε_d is far below the Fermi surface, and $\varepsilon_d + U$ far above. This allows us to introduce the quantities

$$J_{12} = \frac{2V^2}{\Omega} \sum_{\mathbf{k}} \frac{1}{\varepsilon_{\mathbf{k}} - \varepsilon_d - U}, \quad J_{10} = \frac{2V^2}{\Omega} \sum_{\mathbf{k}} \frac{1}{\varepsilon_{\mathbf{k}} - \varepsilon_d}$$

and write

$$\frac{i}{2} [S, \mathcal{H}_h] = -\frac{1}{2\Omega} \sum_{kk'} [J_{12} \mathcal{H}_{12}(\mathbf{k}) \mathcal{H}_{21}(\mathbf{k}') - J_{10} \mathcal{H}_{10}(\mathbf{k}) \mathcal{H}_{01}(\mathbf{k}')].$$

Next we consider how products of operators affect the states of the impurity spin and of the conduction electrons, namely,

$$\begin{aligned} \mathcal{H}_{12}(\mathbf{k}') \mathcal{H}_{21}(\mathbf{k}) &= \sum_{\sigma} \left[n_{\bar{\sigma}} c_{\mathbf{k}'\sigma}^{\dagger} d_{\sigma} n_{\bar{\sigma}} d_{\sigma}^{\dagger} c_{\mathbf{k}\sigma} + n_{\sigma} c_{\mathbf{k}'\bar{\sigma}}^{\dagger} d_{\bar{\sigma}} n_{\bar{\sigma}} d_{\sigma}^{\dagger} c_{\mathbf{k}\sigma} \right] \\ &= \sum_{\sigma} \left[n_{\bar{\sigma}} (1 - n_{\sigma}) c_{\mathbf{k}'\sigma}^{\dagger} c_{\mathbf{k}\sigma} - d_{\sigma}^{\dagger} d_{\bar{\sigma}} c_{\mathbf{k}'\bar{\sigma}}^{\dagger} c_{\mathbf{k}\sigma} \right] = (2 \leftrightarrow 1) \\ \mathcal{H}_{10}(\mathbf{k}) \mathcal{H}_{01}(\mathbf{k}') &= \sum_{\sigma} \left[(1 - n_{\bar{\sigma}}) d_{\sigma}^{\dagger} c_{\mathbf{k}'\sigma} (1 - n_{\bar{\sigma}}) c_{\mathbf{k}\sigma}^{\dagger} d_{\sigma} + (1 - n_{\sigma}) d_{\bar{\sigma}}^{\dagger} c_{\mathbf{k}'\bar{\sigma}} (1 - n_{\bar{\sigma}}) c_{\mathbf{k}\sigma}^{\dagger} d_{\sigma} \right] \\ &= \sum_{\sigma} \left[-n_{\sigma} (1 - n_{\bar{\sigma}}) c_{\mathbf{k}\sigma}^{\dagger} c_{\mathbf{k}'\sigma} - d_{\sigma}^{\dagger} d_{\sigma} c_{\mathbf{k}\sigma}^{\dagger} c_{\mathbf{k}'\bar{\sigma}} \right] = (1 \leftrightarrow 0). \end{aligned} \quad (24.27)$$

Recalling that $n_{\uparrow} (1 - n_{\downarrow}) = 1/2 + S^z$ and $n_{\downarrow} (1 - n_{\uparrow}) = 1/2 - S^z$, we can write

$$\begin{aligned} (2 \leftrightarrow 1) &= n_{\downarrow} (1 - n_{\uparrow}) c_{\mathbf{k}'\uparrow}^{\dagger} c_{\mathbf{k}\uparrow} - d_{\uparrow}^{\dagger} d_{\downarrow} c_{\mathbf{k}'\downarrow}^{\dagger} c_{\mathbf{k}\uparrow} + n_{\uparrow} (1 - n_{\downarrow}) c_{\mathbf{k}'\downarrow}^{\dagger} c_{\mathbf{k}\downarrow} - d_{\downarrow}^{\dagger} d_{\uparrow} c_{\mathbf{k}'\uparrow}^{\dagger} c_{\mathbf{k}\downarrow} \\ &= \left(\frac{1}{2} - S^z \right) c_{\mathbf{k}'\uparrow}^{\dagger} c_{\mathbf{k}\uparrow} - S^+ c_{\mathbf{k}'\downarrow}^{\dagger} c_{\mathbf{k}\uparrow} + \left(\frac{1}{2} + S^z \right) c_{\mathbf{k}'\downarrow}^{\dagger} c_{\mathbf{k}\downarrow} - S^- c_{\mathbf{k}'\uparrow}^{\dagger} c_{\mathbf{k}\downarrow} \\ &= \frac{1}{2} (c_{\mathbf{k}'\uparrow}^{\dagger} c_{\mathbf{k}\uparrow} + c_{\mathbf{k}'\downarrow}^{\dagger} c_{\mathbf{k}\downarrow}) - 2S \cdot c_{\mathbf{k}'\sigma'}^{\dagger} \mathbf{s}^{\sigma'\sigma} c_{\mathbf{k}\sigma} \end{aligned} \quad (24.28)$$

and

$$(1 \leftrightarrow 0) = -\frac{1}{2} (c_{\mathbf{k}'\uparrow}^{\dagger} c_{\mathbf{k}\uparrow} + c_{\mathbf{k}'\downarrow}^{\dagger} c_{\mathbf{k}\downarrow}) - 2S \cdot c_{\mathbf{k}'\sigma'}^{\dagger} \mathbf{s}^{\sigma'\sigma} c_{\mathbf{k}\sigma},$$

where $\mathbf{s} = \frac{\hbar}{2} \boldsymbol{\sigma}$, with $\boldsymbol{\sigma}$ being the Pauli matrix.

The sum of these terms produces two distinct scattering channels:

- A spin-independent scattering channel, carrying regular impurity disorder scattering, with a coefficient $J_{10} + J_{12}$
- A second channel containing the exchange interaction of the impurity spin with the conduction electrons with a coefficient $J_{10} - J_{12}$

Here we are interested in the second channel, which yields the Kondo Hamiltonian

$$\mathcal{H}_{\text{Kondo}} = \sum_{\mathbf{k}\sigma} \varepsilon_{\mathbf{k}\sigma} c_{\mathbf{k}\sigma}^\dagger c_{\mathbf{k}\sigma} + \frac{J}{\Omega} \mathbf{S} \cdot \sum_{\substack{\mathbf{k}\mathbf{k}' \\ \sigma\sigma'}} c_{\mathbf{k}'\sigma'}^\dagger \mathbf{S}^{\sigma'\sigma} c_{\mathbf{k}\sigma}, \quad (24.29)$$

where

$$J = J_{10} - J_{12} = \frac{2V^2}{\Omega} \sum_{\mathbf{k}} \frac{-U}{(\varepsilon_{\mathbf{k}} - \varepsilon_d - U)(\varepsilon_{\mathbf{k}} - \varepsilon_d)} \approx -\frac{2V^2}{\Omega} \frac{U}{\varepsilon_d(\varepsilon_d + U)}$$

$$J \approx -\frac{2V^2}{\Omega} \frac{1}{\varepsilon_d}, \quad U \gg \varepsilon_d \quad \text{Strong repulsion limit.}$$

J is clearly positive, since $\varepsilon_d < 0$ and $\varepsilon_d + U > 0$. Thus we find that the localized spin couples to the spins of the conduction electrons that overlap it. Such coupling can cause spin-flips and may enhance the scattering. We also note that the coupling is antiferromagnetic, which favors the formation of a singlet; however, this competes with the kinetic energy cost of single occupation of conduction electron levels.

24.5 The Kondo Effect

Normally the resistance of pure metals monotonically decreases as the temperature is lowered, as electronic inelastic scattering processes, mainly due to phonons, are suppressed. Adding impurities is expected to give rise to a constant offset that does not change the monotonicity. But, the story of the Kondo effect starts in the 1930s, when de Haas and coworkers [48] in Leiden measured the resistance of some metals at very low temperatures. Surprisingly, they found that gold samples' resistance increased rather than decreased upon cooling down below $\sim 8\text{K}$, as shown in Figure 24.18. Subsequently, it was realized that alloys containing dilute magnetic moments, such as a low concentration of Mn or Fe in Cu, sometimes show similar trends. An explanation of the minimum was given by Kondo in 1964, but it took a further decade before the nature of the ground state was properly understood, and it was only in 1980 that a model for the phenomenon was solved exactly.

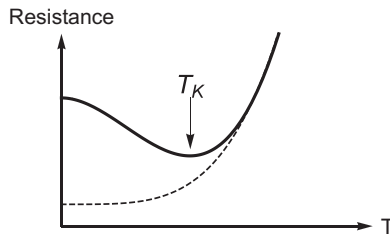


Figure 24.18 Electrical resistance of an alloy exhibiting the Kondo effect.

24.5.1 The Kondo Model

The mean field (Hartree–Fock) approximation to the Anderson model provided an explanation for the local moment formation at magnetic impurity sites in nonmagnetic metallic hosts. However, it failed to predict the strange behavior at low temperatures and low energies that should be manifest in the model. A primary example is the peculiar disappearance of the moments at low temperatures, where they become effectively screened by the conduction electrons. The disappearance is found to be associated with one quasielectron effectively binding with the impurity moment to create a local singlet state that behaves like a nonmagnetic scatterer, at $T = 0$. This physical picture was proposed by Kondo, in his attempt to explain the existence of the resistance minimum described previously. Kondo treated the problem perturbatively in terms of an exchange coupling between the magnetic impurity and the conduction band. The Hamiltonian constructed by Kondo is

$$\mathcal{H}_K = \sum_{\mathbf{k}\sigma} \varepsilon_{\mathbf{k}\sigma} c_{\mathbf{k}\sigma}^\dagger c_{\mathbf{k}\sigma} + \mathcal{H}_s = \sum_{\mathbf{k}\sigma} \varepsilon_{\mathbf{k}\sigma} c_{\mathbf{k}\sigma}^\dagger c_{\mathbf{k}\sigma} + J \mathbf{S} \cdot \mathbf{s}(0), \quad (24.30)$$

where \mathbf{S} represents the local impurity moment and $\mathbf{s}(0)$ is the spin density of the conduction electrons at the impurity site. It is in fact identical to (24.29), when we can write the exchange interaction as

$$\begin{aligned} \mathcal{H}_s &= J \mathbf{S} \cdot \mathbf{s}(0) = J \left[S^z s^z(0) + \frac{1}{2} (S^+ s^-(0) + S^- s^+(0)) \right] \\ &= \frac{J}{\Omega} \sum_{\mathbf{k}\mathbf{k}'} \left[S^z (c_{\mathbf{k}'\uparrow}^\dagger c_{\mathbf{k}\uparrow} - c_{\mathbf{k}'\downarrow}^\dagger c_{\mathbf{k}\downarrow}) + S^+ c_{\mathbf{k}'\downarrow}^\dagger c_{\mathbf{k}\uparrow} + S^- c_{\mathbf{k}'\uparrow}^\dagger c_{\mathbf{k}\downarrow} \right]. \end{aligned} \quad (24.31)$$

We now follow Kondo's perturbative scheme by adiabatically turning on \mathcal{H}_s in a system that consists of a Fermi sea $|FS\rangle$ and an extra electron at the Fermi level, together with the impurity level. The initial state is then $|i\rangle = c_{\mathbf{k}_i\sigma}^\dagger |FS\rangle$. We determine the scattering amplitude, with the aid of the \mathcal{T} -matrix, between $|i\rangle$ and $|f\rangle = c_{\mathbf{k}_f\sigma'}^\dagger |FS\rangle$,

$$\langle f | \mathcal{T} | i \rangle = 2\pi i \left\langle f \left| \mathcal{H}_s + \mathcal{H}_s \frac{1}{\varepsilon_{\mathbf{k}} - \mathcal{H}_0} \mathcal{H}_s + \dots \right| i \right\rangle.$$

Since we are interested in scattering events that contribute to the resistivity, we have to consider on-the-energy-shell scattering, where $\varepsilon_{\mathbf{k}_i} = \varepsilon_{\mathbf{k}_f}$.

Scattering Amplitude

We find that in the case of large U , the Anderson model has a built-in local moment. This local moment provides a scattering potential for the conduction electrons that is quite different from a conventional scalar potential: it endows the impurity scatterer with internal degrees of freedom. We will now explore the ramifications of this difference.

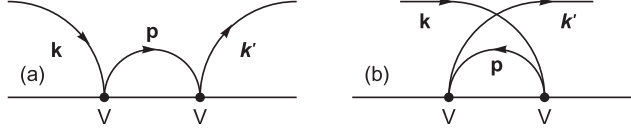


Figure 24.19 Second-order spin-independent scattering processes: (a) direct, (b) exchange.

A. Nonmagnetic Impurity Scattering Pedagogically, it would be instructive to compare the spin-dependent scattering outcome with that of a regular nonmagnetic scattering. We shall first consider the case of a nonmagnetic impurity, with a scattering potential

$$\mathcal{H}_s = \sum_{\mathbf{k}\mathbf{k}',\sigma} c_{\mathbf{k}'\sigma}^\dagger V_{\mathbf{k}\mathbf{k}'} c_{\mathbf{k}\sigma}.$$

We have to consider the direct and exchange channels in second-order processes, as shown in Figure 24.19:

$$\begin{aligned} \left\langle 0 \left| c_{\mathbf{k}_f} c_{\mathbf{k}_f}^\dagger V_{\mathbf{k}_f \mathbf{p}} c_{\mathbf{p}} \frac{1}{\varepsilon_{\mathbf{k}_i} - \mathcal{H}_0} c_{\mathbf{p}}^\dagger V_{\mathbf{p} \mathbf{k}_i} c_{\mathbf{k}_i} c_{\mathbf{k}_i}^\dagger \right| 0 \right\rangle &= V_{\mathbf{k}_f \mathbf{p}} \frac{1 - n_F(\varepsilon_{\mathbf{p}})}{\varepsilon_{\mathbf{k}_i} - \varepsilon_{\mathbf{p}}} V_{\mathbf{p} \mathbf{k}_i} \\ \left\langle 0 \left| c_{\mathbf{k}_f} c_{\mathbf{p}}^\dagger V_{\mathbf{p} \mathbf{k}_i} c_{\mathbf{k}_i} \frac{1}{\varepsilon_{\mathbf{k}_i} - \mathcal{H}_0} c_{\mathbf{k}_f}^\dagger V_{\mathbf{k}_f \mathbf{p}} c_{\mathbf{p}} c_{\mathbf{k}_i}^\dagger \right| 0 \right\rangle &= -V_{\mathbf{p} \mathbf{k}_i} \frac{n_F(\varepsilon_{\mathbf{p}})}{\varepsilon_{\mathbf{k}_i} - (\varepsilon_{\mathbf{k}_i} - \varepsilon_{\mathbf{p}} + \varepsilon_{\mathbf{k}_f})} V_{\mathbf{k}_f \mathbf{p}} \\ &= V_{\mathbf{p} \mathbf{k}_i} \frac{n_F(\varepsilon_{\mathbf{p}})}{\varepsilon_{\mathbf{k}_f} - \varepsilon_{\mathbf{p}}} V_{\mathbf{k}_f \mathbf{p}}. \end{aligned}$$

We note that the first process only takes place if the intermediate state \mathbf{p} is unoccupied, while the second only if it is occupied. Recalling that $\varepsilon_{\mathbf{k}_f} = \varepsilon_{\mathbf{k}_i}$, it is clear that the Fermi function cancels when we take the sum of the two processes. This indicates that there is no significant T dependence to this order in ordinary potential scattering.

B. Magnetic Impurity Scattering Next, we consider the corresponding processes for spin-dependent scattering, where the perturbation is given by \mathcal{H}_s in (24.31). Actually, the exchange interactions of the impurity spin with the conduction electrons produce a correlated choreography, where the impurity spin state at a given time depends on previous scattering events.³ To demonstrate the ensuing effects, we will calculate the scattering amplitude, to second order in J , which will give the scattering rate to $O(J^3)$.

The first-order contribution to the amplitude is

$$\begin{aligned} \langle \mathbf{k}_f \uparrow | \mathcal{H}_s | \mathbf{k}_i \uparrow \rangle &= -\langle \mathbf{k}_f \downarrow | \mathcal{H}_s | \mathbf{k}_i \downarrow \rangle = \frac{JS^z}{\Omega} \\ \langle \mathbf{k}_f \downarrow | \mathcal{H}_s | \mathbf{k}_i \uparrow \rangle &= \frac{JS^+}{\Omega}; \quad \langle \mathbf{k}_f \uparrow | \mathcal{H}_s | \mathbf{k}_i \downarrow \rangle = \frac{JS^-}{\Omega} \end{aligned}$$

³ For example, we consider two electrons, both with spin-up, trying to spin-flip scatter from a spin-down impurity. The first electron can exchange its spin with the impurity and leave it spin-up. The second electron therefore cannot spin-flip scatter because of spin conservation. Thus the electrons of the conduction band cannot be treated as independent objects.

giving a temperature-independent scattering rate of

$$\Gamma \propto \frac{N_{\text{imp}}}{\Omega} \frac{J^2}{\omega} \left[S^z 2 + \frac{1}{2} (S^+ S^- + S^- S^+) \right] \Rightarrow \frac{N_{\text{imp}}}{\Omega} \frac{J^2}{\omega} S(S+1).$$

The second-order contribution is of the form

$$\sum_p \langle \mathbf{k}_f \uparrow | \mathcal{H}_s | p \rangle \frac{1}{\varepsilon - \varepsilon_p} \langle p | \mathcal{H}_s | \mathbf{k}_i \uparrow \rangle,$$

where, again, $\varepsilon = \varepsilon_{\mathbf{k}_i} = \varepsilon_{\mathbf{k}_f}$, and $|p\rangle$ is an intermediate state with energy ε_p . The direct, or non-spin-flip, processes are given by

$$\begin{aligned} \sum_p \langle \mathbf{k}_f \uparrow | S^z c_{\mathbf{k}_f \uparrow}^\dagger c_{\mathbf{p} \uparrow} \frac{1}{\varepsilon - \varepsilon_p} S^z c_{\mathbf{p} \uparrow}^\dagger c_{\mathbf{k}_i \uparrow} | \mathbf{k}_i \uparrow \rangle &= J^2 \sum_{\mathbf{p}} S^z S^z \frac{1 - n_F(\varepsilon_p)}{\varepsilon_{\mathbf{k}_i} - \varepsilon_{\mathbf{p}}} \\ \sum_p \langle \mathbf{k}_f \uparrow | S^z c_{\mathbf{p} \uparrow}^\dagger c_{\mathbf{k}_i \uparrow} \frac{1}{\varepsilon - \varepsilon_p} S^z c_{\mathbf{k}_f \uparrow}^\dagger c_{\mathbf{p} \uparrow} | \mathbf{k}_i \uparrow \rangle &= J^2 \sum_{\mathbf{p}} S^z S^z \frac{n_F(\varepsilon_p)}{\varepsilon_{\mathbf{k}_f} - \varepsilon_{\mathbf{p}}}. \end{aligned}$$

We thermal-average over the intermediate state, by setting

$$c_{\mathbf{p} \downarrow}^\dagger c_{\mathbf{p} \downarrow} \rightarrow \langle c_{\mathbf{p} \downarrow}^\dagger c_{\mathbf{p} \downarrow} \rangle = n_F(\varepsilon_p), \quad \text{and} \quad c_{\mathbf{p} \downarrow} c_{\mathbf{p} \downarrow}^\dagger \rightarrow \langle c_{\mathbf{p} \downarrow} c_{\mathbf{p} \downarrow}^\dagger \rangle = 1 - n_F(\varepsilon_p).$$

Upon adding the two longitudinal contributions, as shown in Figure 24.20, the Fermi distribution cancels out: the final probability does not depend on the occupation of intermediate states and hence on temperature.

The interesting contributions involving spin-flips, shown in Figure 24.21, arise from the processes

$$\begin{aligned} \sum_p \langle \mathbf{k}_f \uparrow | S^- c_{\mathbf{k}_f \uparrow}^\dagger c_{\mathbf{p} \downarrow} \frac{1}{\varepsilon - \varepsilon_p} S^+ c_{\mathbf{p} \downarrow}^\dagger c_{\mathbf{k}_i \uparrow} | \mathbf{k}_i \uparrow \rangle &= J^2 \sum_{\mathbf{p}} S^- S^+ \frac{1 - n_F(\varepsilon_p)}{\varepsilon_{\mathbf{k}_i} - \varepsilon_{\mathbf{p}}} \\ \sum_p \langle \mathbf{k}_f \uparrow | S^+ c_{\mathbf{p} \downarrow}^\dagger c_{\mathbf{k}_i \uparrow} \frac{1}{\varepsilon - \varepsilon_p} S^- c_{\mathbf{k}_f \uparrow}^\dagger c_{\mathbf{p} \downarrow} | \mathbf{k}_i \uparrow \rangle &= J^2 \sum_{\mathbf{p}} S^+ S^- \frac{n_F(\varepsilon_p)}{\varepsilon_{\mathbf{k}_f} - \varepsilon_{\mathbf{p}}}. \end{aligned}$$

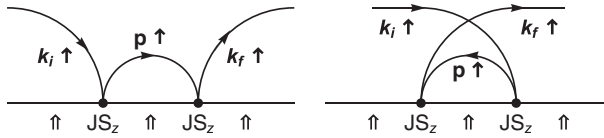


Figure 24.20 Longitudinal terms.

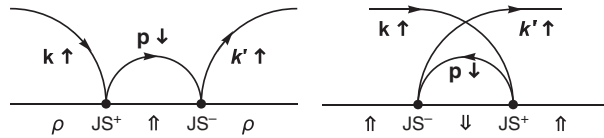


Figure 24.21 Transverse terms.

Combining terms, we then have contributions to the amplitude of

$$\begin{aligned}
 & \frac{J^2}{\Omega} \sum_{\mathbf{p}} \frac{1}{\varepsilon_{\mathbf{k}} - \varepsilon_{\mathbf{p}}} [S^+ S^- n_F(\varepsilon_{\mathbf{p}}) + S^- S^+ (1 - n_F(\varepsilon_{\mathbf{p}}))] \\
 &= S^- S^+ \frac{J^2}{\Omega} \sum_{\mathbf{p}} \frac{1}{\varepsilon_{\mathbf{k}} - \varepsilon_{\mathbf{p}}} + [S^+, S^-] \frac{J^2}{\Omega} \sum_{\mathbf{p}} \frac{n_F(\varepsilon_{\mathbf{p}})}{\varepsilon_{\mathbf{k}} - \varepsilon_{\mathbf{p}}} \\
 &= S^- S^+ \frac{J^2}{\Omega} \sum_{\mathbf{p}} \frac{1}{\varepsilon_{\mathbf{k}} - \varepsilon_{\mathbf{p}}} + \frac{J^2 S^z}{\Omega} \sum_{\mathbf{p}} \frac{n_F(\varepsilon_{\mathbf{p}})}{\varepsilon_{\mathbf{k}} - \varepsilon_{\mathbf{p}}}.
 \end{aligned}$$

The factor $[\varepsilon_{\mathbf{k}} - \varepsilon_{\mathbf{p}}]^{-1}$ in the sums on the right-hand side is divergent at the energy $\varepsilon_{\mathbf{k}}$ of the particle whose scattering amplitude we are calculating, which in the case of most interest is the Fermi energy. For the first sum, this divergence is not important, since contributions from above and below the Fermi energy cancel to leave a finite result. But in the second term, the Fermi function limits this cancellation.

In evaluating the sum over the intermediate states \mathbf{p} in the second term, we assume a conduction bandwidth $[-W, W]$ and a flat density of states \mathcal{D} , and we obtain

$$\begin{aligned}
 \sum_{\mathbf{p}} \frac{n_F(\varepsilon_{\mathbf{p}})}{\varepsilon_{\mathbf{k}} - \varepsilon_{\mathbf{p}}} &\simeq \mathcal{D} \int_{-W}^W d\varepsilon_{\mathbf{p}} \frac{n_F(\varepsilon_{\mathbf{p}})}{\varepsilon_{\mathbf{k}} - \varepsilon_{\mathbf{p}}} \\
 &= \mathcal{D} \left(\ln |W + \varepsilon_{\mathbf{k}}| + \int_{-W}^W d\varepsilon_{\mathbf{p}} \left(-\frac{\partial n_F(\varepsilon_{\mathbf{p}})}{\partial \varepsilon_{\mathbf{p}}} \right) \ln [\varepsilon_{\mathbf{k}} - \varepsilon_{\mathbf{p}}] \right). \quad (24.32)
 \end{aligned}$$

In the last integral, we can approximate the factor of order $\partial n_F / \partial \varepsilon_{\mathbf{p}}$ as finite only in the range $k_B T$, as shown in Figure 24.22, giving

$$\begin{cases} \ln \varepsilon_{\mathbf{k}} & \text{for } \varepsilon_{\mathbf{k}} > k_B T \\ \ln \left[\frac{W}{k_B T} \right] + \text{const.} & \text{for } \varepsilon_{\mathbf{k}} < k_B T. \end{cases}$$

We obtain

$$\frac{1}{\Omega} \sum_{\mathbf{q}} \frac{n_F(\varepsilon_{\mathbf{q}})}{\varepsilon_{\mathbf{k}} - \varepsilon_{\mathbf{q}}} = \mathcal{D}(\varepsilon_F) \ln \left[\frac{W}{k_B T} \right].$$

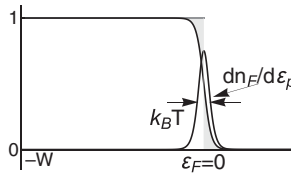


Figure 24.22 Fermi function and its derivative.

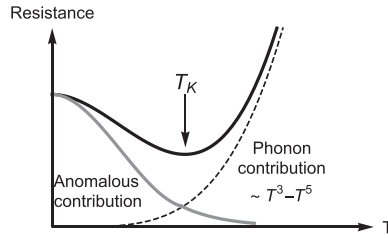


Figure 24.23 Anomalous scattering contribution to the resistivity due to magnetic impurities.

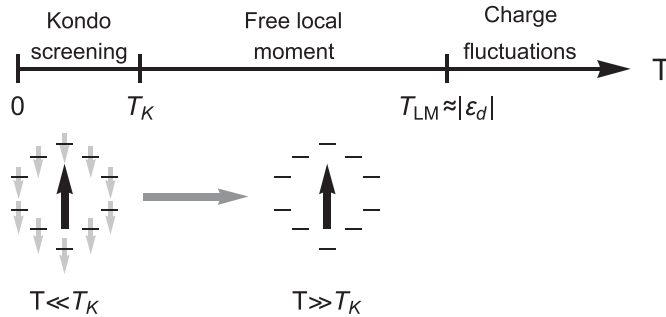


Figure 24.24 Magnetic impurity moment screening above and below the Kondo temperature.

To calculate the scattering rate, we square the combination of the first- and second-order contributions to the amplitude. We find a result proportional to

$$J^2 + 3J^3 \mathcal{D}(\varepsilon_F) \ln \left[\frac{W}{k_B T} \right].$$

which grows with decreasing temperature. Thus, the spin part of the interaction, to a first approximation, makes a contribution to the resistance of order $J^3 \ln(1/T)$. Combined with the phonon contribution to the electron scattering rate, this yields a minimum in the resistance as a function of temperature, as shown in Figure 24.23, for alloys containing magnetic impurities, which is the quest of the Kondo effect.

The temperature scale at which the logarithmic term becomes important is the Kondo temperature $T_K = W e^{-1/2\mathcal{D}J}$, as shown in Figure 24.24. For the physically relevant regime in which $J\mathcal{D}(\varepsilon_F)$ is small, $T_K \ll W$.

We might speculate that when Kondo found this result he might have said “*eureka*,” I found it: a contribution to the resistivity that grows as T gets small. Yet, he might also have realized that at temperatures $T \ll T_K$, the divergence of this contribution signals that perturbation theory is breaking down. Thus we arrive at the realization that even though we are dealing with a single impurity, the Kondo problem is actually a complicated many-body case. Once more we encounter a very singular problem where we have to find a way to sum all the processes.

24.5.2 Variational Approach to the Kondo Problem

Due to the breakdown of perturbation theory with the appearance of a logarithmic singularity in the electron local moment scattering amplitude, we must seek a different approach to analyzing the Kondo S -(d/f) model. In our pursuit to reveal and understand the nature of the Kondo ground state, we should contemplate the case of strong coupling limit in which $J\mathcal{D}(\varepsilon_F)$ is large, namely, an antiferromagnetic J where the impurity spin binds a conduction electron into a singlet state.

To study this scenario, we shall employ a variational method, starting with the trial wave function [187, 205]

$$|\psi_0\rangle = \left[\alpha_0 + \sum_{\mathbf{k} < k_F, \sigma} \alpha_{\mathbf{k}} d_{\sigma}^{\dagger} c_{\mathbf{k}\sigma} \right] \prod_{\mathbf{k} \leq k_F} (c_{\mathbf{k}\uparrow}^{\dagger} c_{\mathbf{k}\downarrow}^{\dagger}) |0\rangle, \quad (24.33)$$

where $\prod_{\mathbf{k} \leq k_F} (c_{\mathbf{k}\uparrow}^{\dagger} c_{\mathbf{k}\downarrow}^{\dagger}) |0\rangle$ represents the filled Fermi sea ground state of the pure system. The first term is just the amplitude for a filled Fermi sea and an empty d/f -state, while the second term is a superposition of states with a filled impurity d/f -level and a hole in the Fermi sea at momentum \mathbf{k} . Actually, the amplitude α_0 is found to be very small, but it does signal a nonzero probability of finding the d/f -level empty, which leaves a striking footprint in the resultant spectrum. The more obvious feature of this trial state wavefunction is that it represents a spin singlet state, shown in Figure 24.25, rather than a single-spin doublet that we would have naively expected.

To calculate the variational energy of the trial wavefunction, we use the variational energy functional

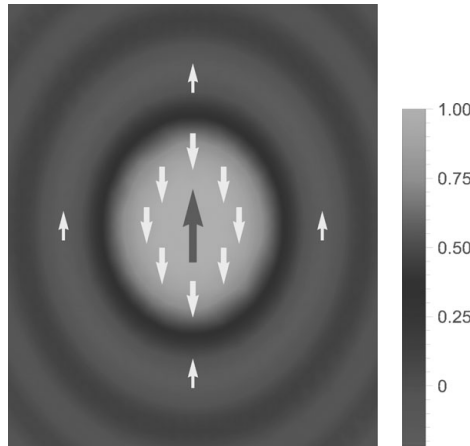


Figure 24.25 Singlet state in the Kondo regime, showing the Kondo cloud.

$$\begin{aligned}
\tilde{E}[\psi_0] &= \langle \psi_0 | \mathcal{H}_A | \psi_0 \rangle - \varepsilon \langle \psi_0 | \psi_0 \rangle \\
\langle \psi_0 | \psi_0 \rangle &= |\alpha_0|^2 + 2 \sum_{\mathbf{k}} |\alpha_{\mathbf{k}}|^2 \\
\langle \psi_0 | \mathcal{H}_A | \psi_0 \rangle &= |\alpha_0|^2 \mathcal{E}_0 + 2 \sum_{\mathbf{k}} |\alpha_{\mathbf{k}}|^2 (\mathcal{E}_0 + \varepsilon_d - \varepsilon_{\mathbf{k}}) + 2V \sum_{\mathbf{k}} [\alpha_0^* \alpha_{\mathbf{k}\sigma} + \alpha_{\mathbf{k}\sigma}^* \alpha_0],
\end{aligned}$$

where ε is a Lagrange multiplier for the normalization condition. We shall measure all energies in the Hamiltonian relative to the Fermi sphere and set $\mathcal{E}_0 = 0$ and take the coefficients to be real. The extremum conditions become

$$\begin{aligned}
\frac{\partial}{\partial \alpha_0} &\Rightarrow 2V \sum_{\mathbf{k}} \alpha_{\mathbf{k}} = \varepsilon \alpha_0 \\
\frac{\partial}{\partial \alpha_{\mathbf{k}}} &\Rightarrow (\varepsilon_d - \varepsilon_{\mathbf{k}}) \alpha_{\mathbf{k}} + V \alpha_0 = \varepsilon \alpha_{\mathbf{k}}.
\end{aligned} \tag{24.34}$$

The solution of (24.34) yields the self-consistent equation

$$\varepsilon = 2 \sum_{k < k_F} \frac{V^2}{\varepsilon - \varepsilon_d + \varepsilon_{\mathbf{k}}}. \tag{24.35}$$

We introduce the binding energy $\Delta_K = \varepsilon - \varepsilon_d < 0$, which provides a measure of the energy of the Kondo singlet trial wavefunction to be compared with that of the singly occupied d/f -state plus the filled Fermi sea configuration ($\mathcal{E}_0 + \varepsilon_d = \varepsilon_d$). This allows us to write (24.35) as

$$\varepsilon_d + \Delta_K = 2 \sum_{k < k_F} \frac{V^2}{\Delta_K + \varepsilon_{\mathbf{k}}} = 2 \sum_{k < k_F} \frac{V^2}{\Delta_K - |\varepsilon_{\mathbf{k}}|}, \tag{24.36}$$

where in the last line we used the fact that $\varepsilon_{\mathbf{k}} < 0$ since the only available states are those below the Fermi surface. Next we change the sum to an integral, setting $|\varepsilon_{\mathbf{k}}| = \mathcal{E}$, and we write

$$\varepsilon_d + \Delta_K = 2 \mathcal{D}(0) \int_0^{\varepsilon_F} d\mathcal{E} \frac{-V^2}{\mathcal{E} - \Delta_K} = 2 \mathcal{D}(0) V^2 \ln \left[\frac{\varepsilon_F}{|\Delta_K|} \right]. \tag{24.37}$$

We note that this result resembles the BCS self-consistent problem, showing a logarithmically divergent behavior at low energies. When the binding energy $|\Delta_K| \ll \varepsilon_d$, we can neglect Δ_K on the left-hand side and rearrange to get

$$\Delta_K = -\varepsilon_F \exp \left[-\frac{1}{2 \mathcal{D}(0) V^2 / \varepsilon_d} \right]. \tag{24.38}$$

But V^2 / ε_d is just the value of the coupling constant J in the Kondo Hamiltonian, and we write

$$\Delta_K = -\varepsilon_F \exp \left[-\frac{1}{2 \mathcal{D}(0) J} \right] < 0. \tag{24.39}$$

This result supports the validity of our singlet ground state represented by our trial wavefunction. We can attribute the emergence of a logarithmic singularity in our results to the possibility of making hole excitations with arbitrarily low energy. Such low-energy excitations are available because of the presence of a sharp Fermi surface and the absence of an energy gap. Thus it becomes easy to induce low-energy excitations, in order to gain the hybridization energy.

There are thus two very different energy scales associated with the original Anderson problem ($\sim \varepsilon_d$) and with the Kondo problem $k_B T_K \sim \varepsilon_d \exp[-1/2\mathcal{D}(0)J]$. The Kondo temperature can become small, particularly when J is small, and a typical scale is around 10°K. Since this is relatively low, it becomes relevant to ask what occurs at temperatures where a localized moment exists, but the Kondo singlet is thermally dissociated, which we will address next.

d/f-Level Occupation

Within the scenario of large U and $\varepsilon_d < 0$, the occupation of the impurity state $\langle n_d \rangle \sim 1$. Thus, it is more instructive to compute

$$1 - \langle n_d \rangle = \frac{\alpha_0^2}{\alpha_0^2 + 2 \sum_{k < k_F} \alpha_{\mathbf{k}}^2} = \frac{1}{1 + 2 \sum_{k < k_F} \left(\frac{\alpha_{\mathbf{k}}}{\alpha_0} \right)^2}. \quad (24.40)$$

We find from (24.34) that

$$\left(\frac{\alpha_{\mathbf{k}}}{\alpha_0} \right)^2 = \frac{V^2}{(\Delta_K + \varepsilon_{\mathbf{k}})^2}.$$

Recalling that $\Delta_K, \varepsilon_{\mathbf{k}} < 0$, we write

$$2 \sum_{k < k_F} \left(\frac{\alpha_{\mathbf{k}}}{\alpha_0} \right)^2 = 2 \mathcal{D}(0) \int_0^{\varepsilon_F} d\varepsilon \frac{V^2}{(|\Delta_K| + |\varepsilon|)^2} = 2 \mathcal{D}(0) \frac{V^2}{\Delta_K} = \frac{2}{\pi} \frac{\Delta}{\Delta_K}, \quad (24.41)$$

where Δ is the resonance width of the impurity level. Substitution in (24.40) yields

$$1 - \langle n_d \rangle = \frac{1}{1 + \frac{2\Delta}{\pi\Delta_K}} \simeq \frac{\pi\Delta_K}{\Delta} \ll 1,$$

where we used the experimental quantities $\Delta \sim 0.5$ eV, and $\Delta_K \sim 10^{-3}$ eV.

From this result, we see that the deviation of the d/f -level occupation from unity is very small; in the variational Kondo wavefunction, the d/f -level is nearly singly occupied, but not quite. In the preceding example, we obtained the Hartree–Fock solution to the Anderson model. One key feature of this solution was that it predicted a doublet of degenerate ground states for the system. In contrast, the Kondo variational ground state is a singlet and does not distinguish up- from down-spins.

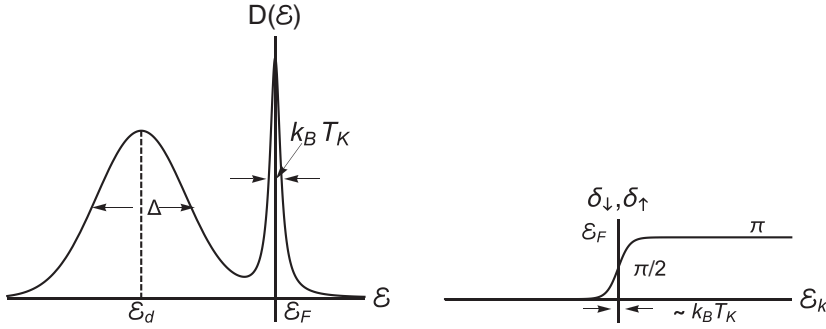


Figure 24.26 For the singlet ground-state function, the excess density of states in the conduction band appears as a Kondo resonance at ε_F , satisfying $\delta_{d\uparrow}(\varepsilon_F) = \delta_{d\downarrow}(\varepsilon_F) \simeq \pi/2$.

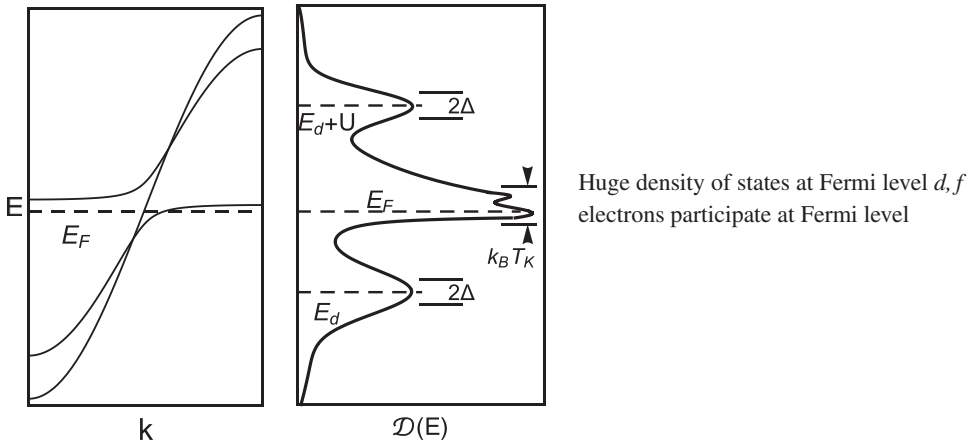


Figure 24.27 Electron dispersions and density of states with $U, V \neq 0$. $k_B T_K$ is the Kondo linewidth, Δ the hybridization parameter, and E_d the ionic d/f energy level.

Kondo Resonance

The result that the d/f -level occupancy is less than unity leads to the presence of extra electron density of states in the conduction band.

Because of the Pauli principle, this excess density of states appears at the Fermi energy and is manifest as a *Kondo resonance peak* of width Δ_K and integrated magnitude of $1 - \langle n_d \rangle = \frac{\pi \Delta_K}{\Delta}$, as shown in Figure 24.26.

We can obtain an alternative physical perspective of this resonance if we consider it through the lens of the Friedel sum rule. We note that the Kondo variational singlet state contains equal probability of up- and down-spin occupation. Moreover, we found that the effective occupation of the d/f -state $\langle n_d \rangle \approx 1$. Consequently, $\langle n_{d\uparrow} \rangle = \langle n_{d\downarrow} \rangle \simeq 1/2$, which, according to the Friedel sum rule, means that at the Fermi energy we have resonances, since $\delta_{d\uparrow} = \delta_{d\downarrow} \simeq \pi/2$. Figure 24.27 shows a typical band dispersion and DOS of a Kondo system."

Exercises

24.1 Spin susceptibility of a superconductor:

Using the Kubo formula, calculate the magnetization $\langle \mu_z \rangle$ of a free Fermi gas associated with an external Zeeman term in the Hamiltonian

$$\mathcal{H}_I = - \int d\mathbf{x}' \mu_z(\mathbf{x}') B_z(\mathbf{x}', t)$$

$$\mu_z(\mathbf{x}) = \mu_B (n_\uparrow(\mathbf{x}) - n_\downarrow(\mathbf{x})).$$

Calculate the spin susceptibility $\chi^{zz}(\mathbf{q}, \omega)$ (follow the Lindhard function derivation in Chapter 7), and show that it is similar to that of the charge susceptibility, up to an overall factor. Show the susceptibility reduces to the Pauli susceptibility, $\chi_{zz}(q \rightarrow 0, \omega = 0, T \rightarrow 0) = \mu_B^2 N_0$.

Repeat the calculation for the superconducting state, and predict the temperature dependence of the Pauli susceptibility for $T \ll T_c$ in that state.

24.2 Frustration:

On a bipartite lattice (i.e., one in which the neighbors of one sublattice belong to the other sublattice), the ground state (known as a Néel state) of a classical antiferromagnet can adopt a staggered spin configuration in which the exchange energy is maximized. Lattices that cannot be classified in this way are said to be frustrated, and the maximal exchange energy associated with each bond cannot be recovered. Using only symmetry arguments, specify one of the possible ground states of a classical three-site triangular lattice antiferromagnet. (Note that the invariance of the Hamiltonian under a global rotation of the spins means that there is manifold continuous degeneracy in the ground state.) Using this result, construct one of the classical ground states of the infinite triangular lattice.

24.3 Commutators in the Anderson model:

Show that the Anderson model Hamiltonian gives

$$[d_\sigma, \mathcal{H}_A] = \varepsilon_d d_\sigma + \sum_{\mathbf{k}} V c_{\mathbf{k}\sigma} + U d_\sigma n_{\bar{\sigma}}.$$

24.4 Ruderman–Kittel–Kasuya–Yosida (RKKY) oscillations:

As we have learned, the RKKY interaction is a mechanism of coupling of localized magnetic moments (nuclear magnetic moments or spins of localized electrons in inner shells) through conduction electrons. The physics of the mechanism is as follows: if we have a localized magnetic moment S , it couples locally to electrons via

$$\mathcal{H}_{\text{int}} = J \mathbf{S} \Psi_\alpha(\mathbf{x}) \sigma_{\alpha\beta} \Psi_\beta(\mathbf{x}).$$

Without loss of generality, assume that $\mathbf{S} \parallel \mathbf{z}$. Then it is equivalent to the potential $\pm JS$ at the position \mathbf{x} for up- and down-spins, respectively. This potential leads to the modulation of density (the actual density, not the density of states!)

$$\delta n_\uparrow(\mathbf{y}) = U(\mathbf{x} - \mathbf{y}) JS, \quad \delta n_\downarrow(\mathbf{y}) = -U(\mathbf{x} - \mathbf{y}) JS$$

with some function $U(\mathbf{x} - \mathbf{y})$. If there is another local spin at the position \mathbf{y} , this modulation of electronic density leads to the interaction between the two magnetic moments given by

$$E_{\text{RKKY}} = 2J^2 \mathbf{S} \cdot \mathbf{S}_2 U(\mathbf{x} - \mathbf{y}).$$

Our goal is to calculate the function $U(\mathbf{x} - \mathbf{y})$. It is a linear response of the density δn at the position \mathbf{y} to the potential at the position \mathbf{x} . Show that this response function is given by the same diagram in Figure 24.9, with the only difference being that now we integrate over the time difference at the positions \mathbf{x} and \mathbf{y} and use the time-ordered Green function. In the frequency representation, it is given by

$$U(R) = \int \frac{d\omega}{2\pi} [G(R, \omega)]^2,$$

where $R = |\mathbf{x} - \mathbf{y}|$. Hint: consider a noninteracting electron gas in the presence of a localized spin S , interacting with the local spin density of electrons. The interaction can be written as

$$\mathcal{H}_1 = J S \delta(\mathbf{x}).$$

Assume that J is small and calculate the spin density of electrons as a function of R the distance to the spin for $R \ll k_F^{-1}$ in the first order in J .